Ectopic expression of a self-incompatibility module triggers growth arrest and cell death in vegetative cells

Lin, Zongcheng; Xie, Fei; Munoz Trivino, Marina; Karimi, Mansour; Bosch, Maurice; Franklin-Tong, Vernonica E.; Nowack, Moritz

Published in:
Plant Physiology

DOI:
10.1104/pp.20.00292

Publication date:
2020

Citation for published version (APA):
Lin, Z., Xie, F., Munoz Trivino, M., Karimi, M., Bosch, M., Franklin-Tong, V. E., & Nowack, M. (2020). Ectopic expression of a self-incompatibility module triggers growth arrest and cell death in vegetative cells. *Plant Physiology*, *183*(2), 1765-1779. https://doi.org/10.1104/pp.20.00292

Short title: *PrpS-PrsS* can act ectopically in vegetative cells

Corresponding authors: Maurice Bosch, Vernonica E. Franklin-Tong, and Moritz K. Nowack

Title: Ectopic expression of a self-incompatibility module triggers growth arrest and cell death in vegetative cells

Zongcheng Lin[a,b], Fei Xie[a,b], Marina Triviño[a,b,c], Mansour Karimi[a,b], Maurice Bosch[c,*], Vernonica E. Franklin-Tong[d,*], and Moritz K. Nowack[a,b,*]

[a] Department of Plant Biotechnology and Bioinformatics, Ghent University, Ghent, 9052, Belgium
[b] Center for Plant Systems Biology, VIB, Ghent, 9052, Belgium
[c] Institute of Biological, Environmental and Rural Sciences (IBERS), Aberystwyth University, Gogerddan, Aberystwyth, SY23 3EB, UK
[d] School of Biosciences, University of Birmingham, Edgbaston, Birmingham, B15 2TT, U.K
[*] Joint corresponding authors

Zongcheng Lin: zolin@psb.vib-ugent.be
Fei Xie: fexie@psb.vib-ugent.be
Marina Triviño: mam124@aber.ac.uk
Mansour Karimi: manka@psb.vib-ugent.be
Maurice Bosch: mub@aber.ac.uk
Vernonica E. Franklin-Tong: v.e.franklin-tong@bham.ac.uk
Moritz K. Nowack: moritz.nowack@vib.be

Joint corresponding authors: v.e.franklin-tong@bham.ac.uk, mub@aber.ac.uk, moritz.nowack@vib.be

Author for contact: Moritz Nowack: moritz.nowack@vib.be

One-sentence summary: *Papaver S*-determinants, which specify self-incompatibility and rejection of self-pollen, trigger growth arrest and programmed cell death in vegetative Arabidopsis tissues when expressed ectopically.

Author contributions
ZL designed, performed the research and analysed data. FX contributed to the live-cell imaging. MT and MK contributed to the vector construction and generation of transgenic lines. ZL, VEF-T, MKN and MB wrote the manuscript.

Revision of submission PP2020-RA-00292

TOC category: **signalling and response**

Key words: *Self-incompatibility (SI), programmed cell death (PCD), cysteine-rich peptide (CRP), calcium, pH, F-actin, DEVDase, evolution*

Abbreviations:
CRP: cysteine-rich peptide;
PCD: programmed cell death;
RLKs: receptor-like kinases;
SAGE: serial analysis of gene expression;
SI: self-incompatibility;
SPHs: S-protein homologues;

Competing interests
The authors declare no conflict of interest.

Materials & Correspondence

Correspondence:
VEF-T: School of Biosciences, College of Life and Environmental Sciences, School of Biosciences, University of Birmingham, Edgbaston, Birmingham, B15 2TT, UK. Email: v.e.franklin-tong@bham.ac.uk; **MB**: Institute of Biological, Environmental and Rural Sciences (IBERS), Aberystwyth University, Gogerddan, Aberystwyth, SY23 3EB, UK. Email: mub@aber.ac.uk; **MN:** Department of Plant Biotechnology and Bioinformatics, Ghent University, Ghent, 9052, Belgium/ Center for Plant Systems Biology, VIB, Ghent, 9052, Belgium Email: moritz.nowack@vib.be.

The authors responsible for distribution of materials integral to the findings presented in this article in accordance with the policy described in the Instructions for Authors: Zongcheng Lin (zolin@psb.vib-ugent.be) and Moritz Nowack (monow@psb.vib-ugent.be).

Funding information:
- European Research Council (ERC) Award Number: 749 639234
- Biotechnology, Biological Sciences Research Council (BBSRC): Award number BB/P005489/1
- FWO: Award numbers G011215N and 12I7417N

Chinese Scholarship Council: Award number: 201806760049.

Abstract

Self-incompatibility (SI) is used by many angiosperms to reject 'self' pollen and avoid inbreeding. In field poppy (*Papaver rhoeas*), SI recognition and rejection of 'self' pollen is facilitated by a female *S*-determinant, *PrsS*, and a male *S*-determinant, *PrpS*. *PrsS* belongs to the cysteine-rich peptide (CRP) family, whose members activate diverse signaling networks involved in plant growth, defense and reproduction. *PrsS* and *PrpS* are tightly regulated and expressed solely in pistil and pollen cells, respectively. Interaction of cognate PrsS and PrpS triggers pollen tube growth inhibition and programmed cell death (PCD) of 'self' pollen. We previously demonstrated functional intergeneric transfer of *PrpS* and *PrsS* to Arabidopsis (*Arabidopsis thaliana*) pollen and pistil. Here we show that *PrpS* and *PrsS*, when expressed ectopically, act as a bipartite module to trigger a 'self-recognition:self-destruct' response in *A. thaliana* independently of its reproductive context, in vegetative cells. Addition of recombinant PrsS to seedling roots expressing the cognate *PrpS* resulted in hallmark features of the *Papaver* SI response, including *S*-specific growth inhibition and PCD of root cells. Moreover, inducible expression of PrsS in *PrpS*-expressing seedlings resulted in rapid death of the entire seedling. This demonstrates that, besides specifying SI, the bipartite PrpS–PrsS module can trigger growth arrest and cell death in vegetative cells. Heterologous, ectopic expression of a plant bipartite signaling module in plants has not been shown previously and, by extrapolation, our findings suggest that CRPs diversified for a variety of specialized functions, including regulation of growth and PCD.

Introduction

Pollen–pistil interactions are complex, crucial events in plant reproductive biology, involving bidirectional signaling between the pistil and the pollen landing on it. Many of the responses regulating pollination take place within the pollen grains, which comprise the highly reduced haploid male gametophyte. The pollen grain is composed of the highly specialized vegetative cell that contains within itself two sperm cells, complete with cell walls and plasma membranes. The pollen's role is to deliver two sperm cells to the embryo sac so that double fertilization can take place. Thus, pollen represents a unique gametophytic structure; for example serial analysis of gene expression (SAGE) studies have revealed that 83% of the pollen-expressed gene tags are pollen-specific and thus thought to have critical functions relating to pollen; see, e.g. (da Costa-Nunes and Grossniklaus, 2003; Honys and Twell, 2004; Mergner et al., 2020).

Self-incompatibility (SI) is an important mechanism used by flowering plants to prevent selfing. It is controlled by a multi-allelic *S*-locus allowing self/non-self-recognition between pistil and pollen. In several SI systems, when male and female *S*-determinant allelic specificities match, self (incompatible) pollen is recognized and rejected before fertilization can occur. A key characteristic of SI determinants is that they are extremely tightly regulated, both in a developmental and tissue-specific manner, being expressed solely in pistil and pollen cells during a narrow developmental window, as the tissues approach maturity (Takayama and Isogai, 2005). SI in poppy (*Papaver rhoeas*) is controlled and specified by *S*-determinants expressed specifically in the stigma (*PrsS* (Foote et al., 1994)) and pollen (*PrpS* (Wheeler et al., 2009)) respectively. *PrpS* encodes a small, novel, integral membrane protein with several predicted transmembrane domains; *PrsS* encodes a small secreted protein, and is the founding member of the large family of S-protein homologs (SPHs), which are found in most dicotyledonous plants, some fungi and metazoa (Rajasekar et al., 2019). This family of small, secreted proteins have features similar to cysteine-rich peptides (CRPs), which include ligands known to be involved in diverse signaling pathways (Bircheneder and Dresselhaus, 2016; Liu et al., 2017; Marshall et al., 2011; Wheeler et al., 2010). However, aside from PrsS, the functional roles of SPHs in plants remains to be established (Rajasekar et al., 2019).

A long-standing model for SI in *Papaver* is that PrsS acts as a signaling ligand to trigger SI in incompatible pollen. While PrpS is distinct from typical plant receptors (e.g. Receptor-Like Kinases (RLKs)), its allele-specific interaction with PrsS activates a network of intracellular signals in incompatible pollen that result in the rapid inhibition of pollen tube growth and ultimately, programmed cell death (PCD). Key hallmark features of *Papaver* SI response include a rapid increase of cytosolic free Ca^{2+} $[Ca^{2+}]_{cyt}$ (Franklin-Tong et al., 1993), a dramatic drop in cytoplasmic pH (Wilkins et al., 2015) and distinctive alterations of the actin cytoskeleton (Geitmann et al., 2000); see (Wang et al., 2019) for a recent review. We previously demonstrated that a cognate PrpS–PrsS interaction in Arabidopsis (*Arabidopsis thaliana*) pollen growing *in vitro* triggered hallmark features of the *Papaver* SI response (de Graaf et al., 2012; Wang et al., 2020) and showed that *PrpS* and *PrsS*, when expressed in pollen and pistil respectively in *A. thaliana*, function to prevent self-seed set, effectively rendering *A. thaliana* self-incompatible (Lin et al., 2015). These findings demonstrated that the *Papaver S*-determinants can be functionally transferred between highly diverged plant species (Bell et al., 2010). However, as the SI response is triggered within the unique, highly specialized context of the pollen, it was unclear whether the PrpS-PrsS module triggers a

pollen-specific pathway, or whether this pair of proteins can trigger growth arrest and cell death pathways in other parts of the plant.

Cellular responses in plants require an integrated signal perception and signal transduction network; such networks are responsible for orchestrating and coordinating a plethora of diverse processes including growth and development. As such, signaling processes allow tissues and organs to communicate with each other efficiently. A major class of proteins involved in cellular communication are those involved in short-range peptide signaling, utilizing small secreted proteins or peptides that act as ligands that interact with some sort of receptors (Sparks et al., 2013). Many signaling peptides are perceived by RLKs and it is thought that much of the specificity of responses is due to localized expression of ligands and their receptors; see (Breiden and Simon, 2016) for a review. For example, although CLAVATA3 CLE family peptides act in both roots and shoots (Fletcher et al., 1999), they nevertheless function in both organs specifically in apical meristematic tissues.

Heterologous expression of plant genes in other plant species has often been used to identify function phenotypically by dominant gene activity (Diener and Hirschi, 2000). Ectopic expression has also been used to demonstrate function; see, for example (Boutilier et al., 2002), who showed that constitutive expression of the BABY BOOM transcription factor promotes cell proliferation and morphogenesis during embryogenesis. However, transfer of two genes encoding a receptor-ligand pair that are normally specifically expressed in certain tissues for a specific function, to a completely different cellular context has, to our knowledge, not previously been explored. Thus far, examples of ectopic expression of single genes in plant cells has typically been restricted to reiterate their function in other cell types to show functional relatedness or to recapitulate an evolutionary divergent event using similar genes from different species. One of the best known examples is perhaps the expression of chimeric ribonuclease genes in anthers of transformed tobacco and oilseed rape plants which specifically destroyed the tapetal cells of developing pollen, resulting in male sterility (Mariani et al., 1990).

Here we have examined the effect of ectopic expression of *PrpS* and *PrsS* from *P. rhoeas* in vegetative cells of *A. thaliana*, using characteristic markers of *Papaver* SI-PCD to examine function. We show that the heterologous, ectopic expression of these genes, which specify a tightly controlled reproductive trait in the male gametophyte, can trigger an “SI-like”

response, resulting in growth arrest and PCD in vegetative sporophytic cells. Ectopic expression of PrpS and PrsS in Arabidopsis vegetative cells recapitulates major cellular aspects of the *Papaver* SI-like response in these cells, providing evidence that this heterologous, bipartite module can signal to similar cellular targets in different cell types.

Results

PrsS treatment results in *S*-specific root growth inhibition of *PrpS*-expressing seedlings

In *Papaver*, interaction of cognate PrpS and PrsS triggers a Ca^{2+}-dependent signaling network in pollen, resulting in a rapid growth arrest followed by PCD of incompatible pollen after SI induction (Franklin-Tong et al., 1997; Franklin-Tong et al., 1995; Franklin-Tong et al., 1993). To examine if the *PrpS-PrsS* module might also work outside the specific context of pollen-pistil interactions, we examined if growth inhibition and PCD caused by the *PrpS-PrsS* module also could be triggered in other tissues. We therefore expressed $PrpS_1$ under a constitutive UBQ10 promoter in *A. thaliana* plants and established five independent single T-DNA insertion lines (*pUBQ10::*$PrpS_1$ line 7/11/12/13/16). RT-qPCR showed that $PrpS_1$ mRNA was substantially expressed in these transgenic *A. thaliana* seedlings (**Fig 1a, Fig S1**). Focusing first on root growth, we did not observe differences in the root length between *A. thaliana* Col-0 wild type (WT) and *pUBQ10::*$PrpS_1$ seedlings (**Fig 1b**), demonstrating that $PrpS_1$ expression alone did not alter seedling development. Next, we applied recombinant $PrsS_1$ protein to 4-day-old root tips of WT and *pUBQ10::*$PrpS_1$ seedlings. Exposure to $PrsS_1$ protein did not show any inhibition effect of normal development and growth of *A. thaliana* WT seedlings (**Fig S2**). However, $PrsS_1$ treatment of *pUBQ10::*$PrpS_1$ seedlings resulted in a rapid and complete inhibition of root growth (**Fig 1b, c**). The growth of *pUBQ10::*$PrpS_1$ seedling roots was inhibited by recombinant $PrsS_1$ protein in a dose-dependent manner (**Fig 1d)**. Treatment of *pUBQ10::*$PrpS_1$ roots with 5 $ng.\mu L^{-1}$ $PrsS_1$ significantly inhibited their growth rate, while ≥10 $ng.\mu L^{-1}$ completely blocked root elongation. This provides evidence that the *PrpS-PrsS* module, although its constitutive components are normally only expressed in pollen and pistil respectively and triggers a response in pollen specifically, can also act to trigger the inhibition of growth of vegetative, sporophytic cells.

S-allele specific inhibition is a key feature of the *Papaver* SI response. To test this, we treated *pUBQ10::*$PrpS_1$ and WT seedlings with either $PrsS_1$ or $PrsS_3$ recombinant protein. *pUBQ10::*$PrpS_1$ seedling roots were strongly inhibited by the $PrsS_1$ protein, while the $PrsS_3$ protein had no effect; WT seedling roots were not inhibited by any treatment (**Fig 1b, c**). As only a cognate *PrpS-PrsS* combination caused growth inhibition, this shows that the *S*-determinants maintain their *S*-specificity in Arabidopsis roots.

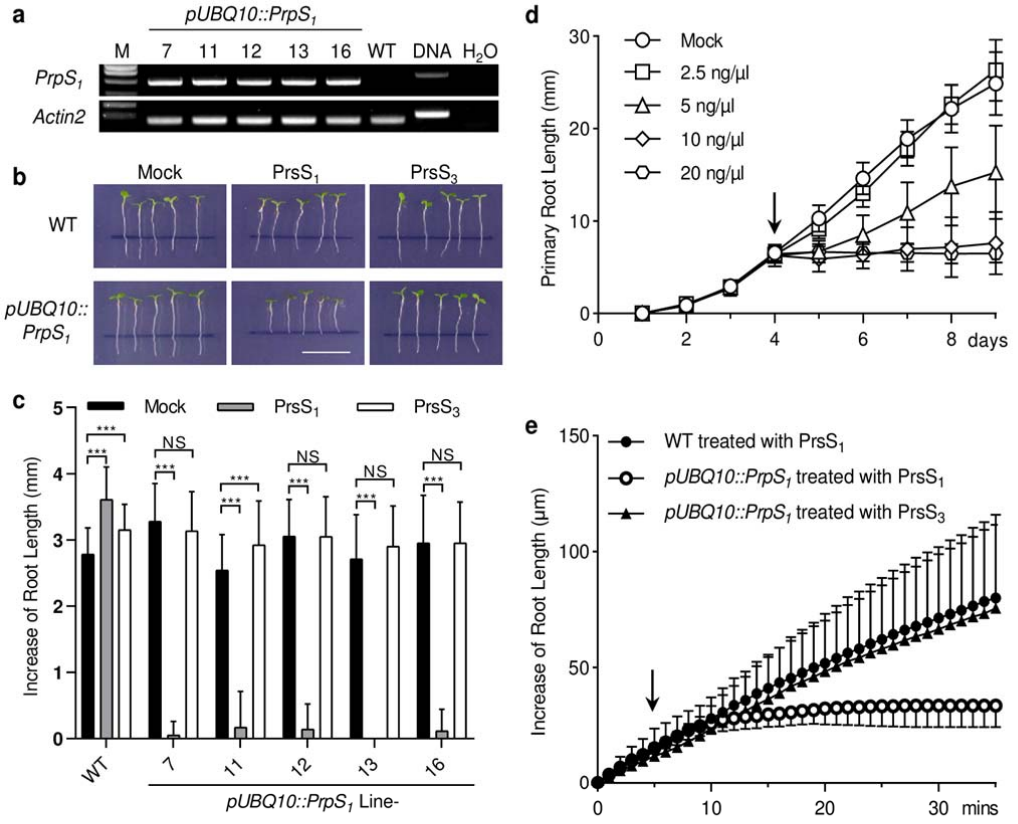

Fig 1. Expression of *PrpS* in transgenic *Arabidopsis thaliana* triggers root growth inhibition after cognate PrsS treatment.

(a) RT-PCR shows the expression of *PrpS*$_1$ mRNA in *pUBQ10::PrpS*$_1$ transgenic seedlings. Expression levels varied. *Actin2* was used as a housekeeping gene control.

(b, c) *S*-specific inhibition of root growth of *pUBQ10::PrpS*$_1$ seedlings after PrsS$_1$ treatment.
(**b**) Images of 4-day-old seedlings 24 h after treatment with PrsS proteins (10 ng.µl^{-1}). Black lines indicate the position of root tips when treated. Only *pUBQ10::PrpS*$_1$ seedlings (line 12) treated with PrsS$_1$ (bottom, centre) display inhibited root growth. This line was used for all the other experiments if not specified. Bar = 1 cm.
(**c**) Quantitation of increases in seedling root length from different transgenic lines (see (a)) treated with PrsS proteins (10 ng.µl^{-1}) 24h after treatment (mean ± SD, n = 20-25 seedlings). All five lines had root growth significantly inhibited by PrsS$_1$ when comparisons were made with either PrsS$_3$ or "mock" treatment for each line (Two-way ANOVA multiple comparison; NS, not significant; ***, p<0.001).

(d) Root growth of *pUBQ10::PrpS*$_1$ seedlings was inhibited by PrsS$_1$ in a dose-dependent manner. X-axis indicates time (days) after transferal of plates to the growth chamber. Arrow indicates when the treatment was added. Result = mean ± SD. N = 20-25 seedlings.

(e) PrsS$_1$ treatment induces rapid root growth inhibition of *pUBQ10::PrpS*$_1$ seedlings in an *S*-specific manner. Arrow indicates the time-point of PrsS addition (10 ng.µl^{-1}). Two-way ANOVA shows PrsS$_1$ treatment significantly inhibited root growth (p<0.001, ***), while PrsS$_3$ did not (p=0.29), in comparison with WT seedlings treated with PrsS$_1$. Result = mean ± SD. N = 6.

As the SI response in pollen triggers rapid inhibition of incompatible pollen tube growth, we examined the timing of inhibition of growth of the roots in more detail, using a perfusion

chamber system in combination with confocal microscopy (Krebs and Schumacher, 2013). Under these conditions, WT seedling roots elongated at a rate of ~2.3 μm.min^{-1}, and addition of PrsS proteins did not affect this (**Fig 1e, Fig S3a, d**). However, addition of $PrsS_1$ protein resulted in a rapid reduction of root growth of *pUBQ10::PrpS$_1$* seedlings ($p<0.001$, two-way ANOVA; **Fig 1e**). Growth was completely inhibited within 5-20 min after addition of $PrsS_1$ (**Fig S3b, e, g**). This inhibition was only observed with a cognate PrpS-PrsS interaction; in a compatible interaction, using the non-cognate recombinant $PrsS_3$ protein, roots of *pUBQ10::PrpS$_1$* seedlings grew at a similar rate to WT roots ($p=0.29$, two-way ANOVA; **Fig 1e, Fig S3c, f**). Taken together, these data demonstrate that PrpS and PrsS interaction in roots rapidly elicits inhibition of growth. This response is strikingly similar to what was observed in *Papaver* pollen tubes during the SI response (Thomas and Franklin-Tong, 2004). However, a key difference is that root is a multicellular organ that increases its length by diffuse growth, whereas the pollen tube is a single cell elongating by tip growth. Together these data demonstrate that the PrpS-PrsS bipartite signaling module can operate ectopically to inhibit growth of vegetative cells.

PrsS triggers cell death and DEVDase activation in *PrpS*-expressing seedlings

In *Papaver* pollen, downstream of PrpS and PrsS interaction, after inhibition of growth, a distinctive PCD programme is triggered. To investigate if this aspect of the SI response could be recapitulated in *PrpS*-expressing Arabidopsis roots, we examined root cells for evidence of death after PrsS treatment. We first examined plasma membrane (PM) permeability using propidium iodide (PI) staining, and nuclear integrity using a nuclear-localized fluorescent protein marker line (*pUBQ10::NLS-YC3.6* (Nagai et al., 2004) containing both nuclear localized eCFP and cpVENUS). Twenty-four hours after addition of $PrsS_1$ to *pUBQ10::PrpS$_1$* seedling root tips, we found that many cells showed PM permeabilization to PI and loss of nuclear integrity, providing evidence of death (**Fig 2a, b**). This occurred in the whole root tip region, including the different cell types in the root cap, the root meristem, transition zone and elongation zone (**Fig 2a, b)**. Examining temporal changes to the root after $PrsS_1$ treatment, we observed a gradual increase in the number of dead cells (**Fig S4**). A significant increase in PI staining was initially observed in the lateral root cap (LRC) 1 h after SI-induction. At 2 h, cell death was observed in the columella root cap region. Cell death in the meristem was observed 4 h after $PrsS_1$ treatment, and the number of cells affected increased over time. In contrast, in the controls (mock-treated and treated with $PrsS_3$), only a few PI-positive cells were observed in the root cap (**Fig 2b, FigS4**), which undergoes PCD

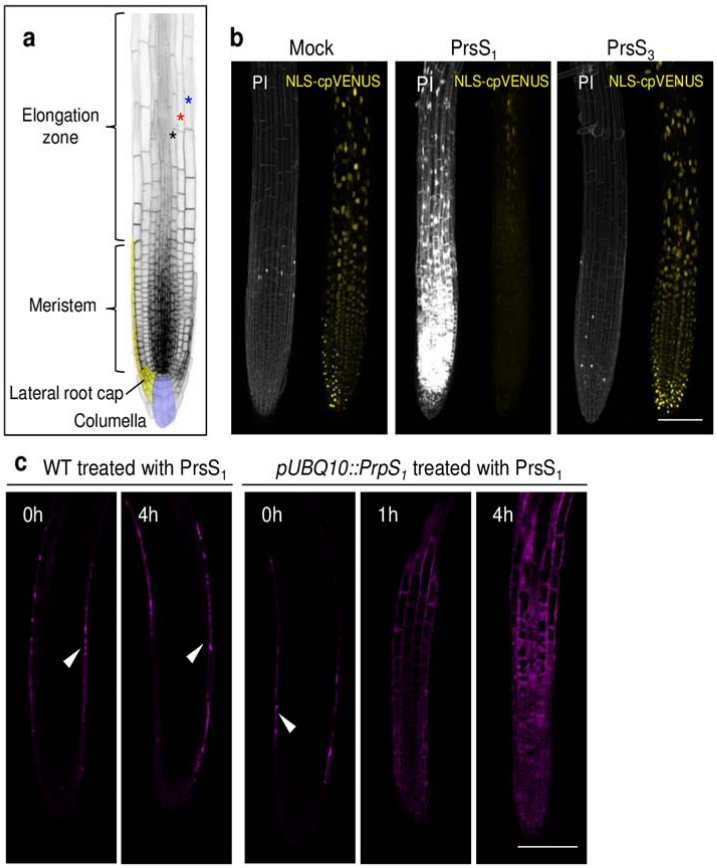

Fig 2. PrsS treatment results in cell death of PrpS-expressing seedling root cells.

(a) An image of a root illustrating different regions of the root tip. Cell files of epidermis, cortex and endodermis are indicated by blue, red and black stars, respectively.

(b) PrsS treatment results in the *S*-specific cell death of *pUBQ10::PrpS$_1$* roots. Representative images of *pUBQ10::PrpS$_1$* roots expressing NLS-YC3.6 stained with PI 24h after treatment (n>6). No death was observed in roots mock-treated with buffer (mock), as shown by the absence of PI staining (PI, left hand images). Cognate $PrsS_1$ treatment (10 ng.µl^{-1}) resulted in high levels of PI staining (white) in *pUBQ10::PrpS$_1$* seedling roots, but those treated with compatible $PrsS_3$ (10 ng.µl^{-1}) did not. The NLS-cpVENUS signal (yellow) also reveals evidence of cell death, as it is lost after cognate $PrsS_1$ addition. Images were taken 24h after treatment. Bar = 100 µm.

(c) PrsS addition activates a DEVDase activity in *pUBQ10::PrpS$_1$* seedling roots. DEVDase activity was monitored using the $CR(DEVD)_2$ probe (purple). Besides endogenous DEVDase activity detected in the lateral root cap (indicated by white triangles), no DEVDase activity was observed in the root tip of WT seedlings before or after $PrsS_1$ (10 ng.µl^{-1}) treatment. For the $PrpS_1$-expressing root, DEVDase activity was observed within 1 h of $PrsS_1$ addition in different cell types including epidermis, cortex and endodermis, of both the meristem and elongation zone of the root tip, and activity subsequently increased further. Representative images (n=5) of single Z-optical sections are shown here; a full projection image is shown in Fig S5. Bar = 100 µm.

261 during root development (Fendrych et al., 2014). These results provide good evidence that

cognate combinations of PrpS-PrsS, besides specifying SI, can operate to trigger cell death in vegetative cells.

To investigate if a similar pathway to that triggered in *Papaver* pollen was utilized in the death of the root cells, as a DEVDase is implicated as a key PCD executor (Bosch and Franklin-Tong, 2007) in *Papaver* pollen SI-PCD, we examined this protease activity in the *pUBQ10::PrpS$_1$* seedling roots. The chemically synthesized probe CR(DEVD)$_2$ was employed to detect DEVDase activity in roots *in vivo*. In WT roots, consistent with the occurrence of normal, constitutive root cap PCD (Fendrych et al., 2014), DEVDase activity was detected in the outermost layer of the root in the root cap prior to treatment (**Fig 2c, Fig S5a**). Addition of PrsS proteins to WT seedling roots did not affect DEVDase activity even after 4h (**Fig 2c, Fig S5a**). However, treatment of *pUBQ10::PrpS$_1$* roots with PrsS$_1$ induced the activation of DEVDase activity in several different zones and cell types, including the root cap, meristem, and elongation zone (**Fig 2c, Fig S5b**). When *pUBQ10::PrpS$_1$* roots were treated with PrsS$_3$ protein, no major differences in DEVDase activity were observed compared to that in untreated roots (**Fig S5c, d**). This demonstrates that DEVDase activation is induced by PrpS-PrsS interaction in these *PrpS$_1$*-expressing Arabidopsis seedling roots and that DEVDase activation is *S*-allele specific in these vegetative tissues. This suggests that a similar pathway is reconstituted in these vegetative cells by this bipartite module.

PrsS treatment triggers an *S*-specific Ca^{2+} signature in *PrpS*-expressing roots

We next investigated whether other hallmark downstream features of the *Papaver* SI response were triggered in the *PrpS*-expressing roots after addition of cognate PrsS proteins. To monitor the cytosolic Ca^{2+} ($[Ca^{2+}]_{cyt}$) spatio-temporally, the genetically encoded calcium indicator *YC3.6* (Krebs et al., 2012; Nagai et al., 2004) was co-expressed with *PrpS$_1$* in Arabidopsis seedlings. We observed no obvious change in the $[Ca^{2+}]_{cyt}$ when WT seedlings were treated with PrsS$_1$ protein (**Fig 3a, Fig S6a**). However, when PrsS$_1$ protein was added to *PrpS$_1$*-expressing seedlings, we detected transient $[Ca^{2+}]_{cyt}$ increases in their roots. The increase was first observed in the elongation zone of the root, peaking ~10 min after PrsS protein addition, and subsequently gradually decreased back to ~resting level within ~25 min (**Fig 3a, Fig S6b**). An increase in $[Ca^{2+}]_{cyt}$ in the meristem and columella regions was also observed (**Fig S6b**). These $[Ca^{2+}]_{cyt}$ dynamics were not observed in *PrpS$_1$*-expressing seedlings treated with PrsS$_3$ protein (**Fig 3a, Fig S6c**), demonstrating that this $[Ca^{2+}]_{cyt}$ response was *S*-specific. We also examined roots for increases in nuclear Ca^{2+} ($[Ca^{2+}]_{nuc}$)

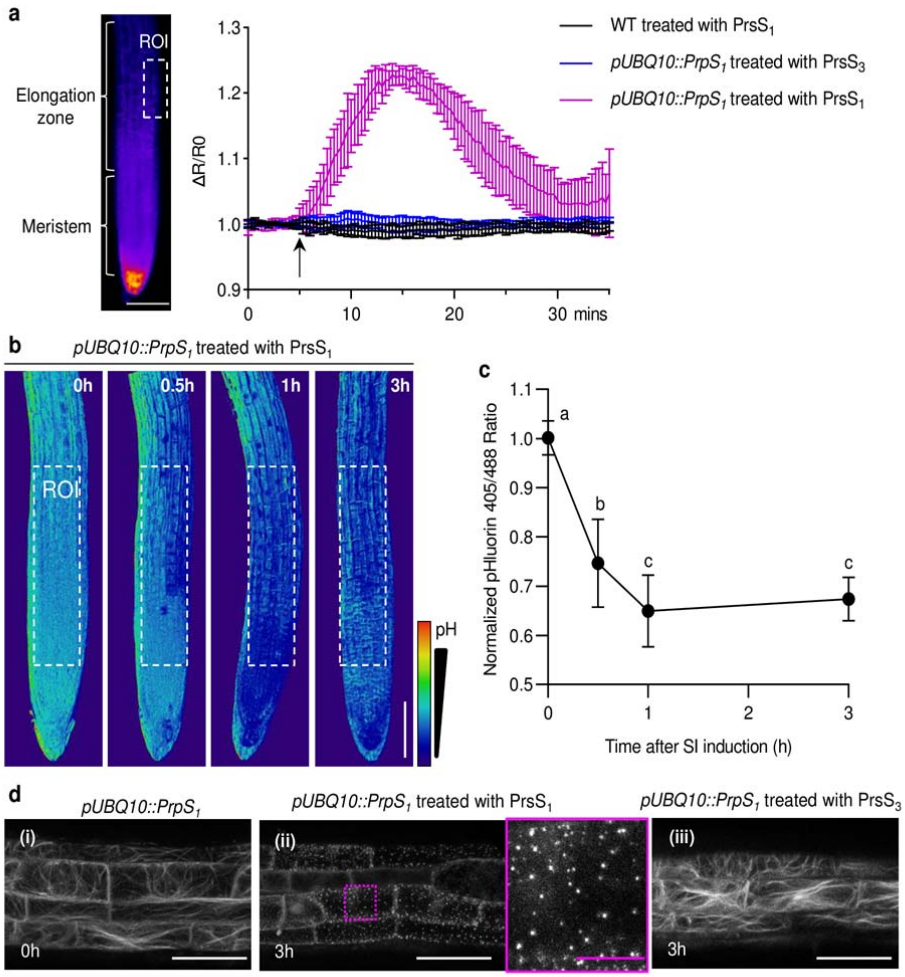

Fig 3. Key hallmarks of *Papaver* SI response are observed in the *Arabidopsis thaliana* PrpS-expressing roots after PrsS induction.

(a) PrsS induces transient increases in cytosolic free Ca^{2+} ($[Ca^{2+}]_{cyt}$) in cognate *PrpS*-expressing Arabidopsis seedling roots. Quantitation of changes in $[Ca^{2+}]_{cyt}$ measured in Arabidopsis seedling roots in the elongation zone (l.h. image ROI, dotted box), using the Ca^{2+} marker YC3.6 signal expressed as fractional ratio changes (ΔR/R0; mean ± SD, n=6). After PrsS addition (10 ng.µl^{-1}, indicated by arrow) an increase in $[Ca^{2+}]_{cyt}$ was observed in in the elongation zone of *pUBQ10::PrpS$_1$* roots treated with $PrsS_1$ (magenta); controls (black, blue) did not display this response.

(b, c) PrsS triggers acidification in cognate PrpS-expressing Arabidopsis seedling root.
(b) Ratiometric (405nm/488nm) imaging of *pUBQ10::PrpS$_1$* roots expressing the pH sensor pHluorin after $PrsS_1$ (10 ng.µl^{-1}) addition revealed that the signal ratio decreased, indicating cytosolic acidification. Bar = 100 µm. (c) Quantification of the pHluorin ratio measured in the ROI (white dotted box in (b)) of these roots shows a significant decrease in $[pH]_{cyt}$ after SI induction (mean ± SD, n=12; one-way ANOVA with multiple comparison test, between a & b, b & c: $p<0.001$; c *vs* c is N.S.). The pHluorin ratio at time = 0 h was normalized to 1.

(d) PrsS treatment triggers *S*-specific loss of actin filaments and formation of actin foci in roots.
Representative images (n>6) of confocal imaging of *pUBQ10::PrpS$_1$* roots (elongation zone) expressing LifeAct-mRuby2. (i) Prior to treatment, typical longitudinal actin filament bundles were observed. (ii) 3 h after treatment with $PrsS_1$ (10 ng.µl^{-1}), actin foci were observed (magenta dotted box and magnification of this region to the right). (iii) The same line at 3 h after addition of $PrsS_3$ proteins (10 ng.µl^{-1}) displayed normal longitudinal actin filament bundles. Images are full projections, white bars = 50 µm, magenta bar = 10 µm.

296 after addition of PrsS, by introducing a NLS-YC3.6 construct into the *pUBQ10::PrpS$_1$*

transgenic seedlings. We observed increases in $[Ca^{2+}]_{nuc}$ at the root tip, including columella, meristem and elongation zone (**Fig S7**), which were spatio-temporally similar to the $[Ca^{2+}]_{cyt}$ response. Our observation of unsynchronized Ca^{2+} signatures in different part of the root hints at possible transmission of Ca^{2+} signaling between neighbouring tissues in the *pUBQ10::PrpS$_1$* root triggered by $PrsS_1$. As increases in $[Ca^{2+}]_{cyt}$ are a key feature of the SI response, our data suggest that we may be observing a "SI-like" response in vegetative tissues.

PrsS induces *S*-specific cytoplasmic acidification in *PrpS*-expressing roots

Another hallmark feature of the *Papaver* SI is cytosolic acidification. We examined *PrpS$_1$*-expressing roots treated with PrsS proteins for alterations in cytoplasmic pH ($[pH]_{cyt}$) using the genetically-encoded pH sensitive GFP variant, pHluorin (Moseyko and Feldman, 2001). After 30 min $PrsS_1$ treatment, $PrpS_1$-expressing roots displayed a significant drop in $[pH]_{cyt}$ in ($p<0.0001$, one-way ANOVA, **Fig 3b, c**). Further cytoplasmic acidification continued until ~1 h, and levels remained low, as the pHluorin 405/488 ratio at 3 h was not significantly different to that at 1 h ($p=0.7975$, one-way ANOVA, **Fig 3b, c**). This rapid drop in $[pH]_{cyt}$ was only observed in *PrpS$_1$*-expressing roots treated with cognate $PrsS_1$ proteins, and not in WT seedlings treated with $PrsS_{1/3}$ proteins, nor $PrpS_1$-expressing roots treated with $PrsS_3$ proteins (**Fig S8**). The temporal pH dynamics after PrpS-PrsS interaction in Arabidopsis root was similar to that observed in *Papaver* pollen after SI induction. These data demonstrate that cognate PrpS-PrsS interaction in Arabidopsis roots induces cytoplasmic acidification, and further supports the idea that a *Papaver* SI-like signaling pathway is triggered in Arabidopsis roots after interaction of cognate PrpS and PrsS.

PrsS triggers actin cytoskeletal remodelling in *PrpS*-expressing seedling roots

As highly characteristic alterations to the actin cytoskeleton are a key feature of *Papaver* SI, we examined the dynamics of actin cytoskeleton to see if this characteristic marker was also utilized in the root response. We added recombinant PrsS to *pUBQ10::PrpS$_1$* transgenic seedling roots that also expressed the genetically encoded actin marker, LifeAct-mRuby2 (Bascom et al., 2018; Dyachok et al., 2014). WT roots displayed typical actin filament bundles before and after $PrsS_1$ application (**Fig S9a**). *PrpS$_1$*-expressing roots showed a similar actin organisation prior to the addition of recombinant $PrsS_1$ (**Fig 3d**). However, by 60 min after $PrsS_1$ application, the mRuby2 signal in the *PrpS$_1$*-expressing seedling roots was much reduced, fragmented actin filaments were detected and small punctate actin foci had

formed (**Fig S9b)**. At 3 h, the actin foci were brighter and larger (**Fig 3d, Fig S9b)**. These distinctive actin alterations are very similar to what has been described for incompatible pollen in the *Papaver* SI response (Snowman et al., 2002). In roots, we also observed abnormally thick actin bundles and actin aggregation around the nucleus at 3 h after cognate PrsS treatment (**Fig S9b**). *PrpS*$_1$-expressing roots did not undergo any actin remodelling after treatment with recombinant PrsS$_3$ protein (**Fig 3d)** demonstrating that actin remodelling is an *S*-specific event. Together, these observations demonstrate that interaction of PrpS and PrsS in Arabidopsis roots triggers a signaling network involving hallmark features observed in incompatible pollen in the *Papaver* SI response (Snowman et al., 2002), suggesting that they can recapitulate a "SI-like" response in vegetative tissues.

PrsS treatment results in an *S*-specific cell death of *PrpS*-expressing leaf protoplasts

As our data suggested that a *Papaver* SI-PCD-like signaling pathway could be triggered in Arabidopsis root cells, we wondered whether this response might also be observed in other somatic cell types. We therefore examined whether the viability of leaf protoplasts derived from *PrpS*$_1$-expressing Arabidopsis plants might also be affected by PrsS$_1$ proteins treatment. We utilized a nuclear-localized eCFP (NLS-eCFP) signal as a cell viability marker for leaf protoplasts. After 8 h incubation with PrsS$_1$ protein, only *PrpS*$_1$-expressing protoplasts showed a loss of the NLS-eCFP signal, together with abnormal cell shape and leakage of cellular contents (**Fig 4a**). In contrast, treatment with PrsS$_3$ protein or mock treatment with buffer had no effect; these control protoplasts appeared viable and intact and the same as untreated WT protoplasts (**Fig 4a**). Quantitative, temporal analysis showed a gradual and significant decrease in the ratio of protoplasts displaying a positive NLS-eCFP signal. Prior to treatment this was 95.7% and it decreased to 71.2% at 1 h ($P<0.05$, one-way ANOVA, **Fig 4b**), progressively decreasing down to 15.6% after 8 h ($P<0.001$, one-way ANOVA, **Fig 4b**). This was not observed in the WT protoplasts or *PrpS*$_1$-expressing protoplast incubated with PrsS$_3$ proteins, which displayed NLS-eCFP signals not significantly different from the untreated controls ($P=0.7532$, one-way ANOVA, **Fig 4b**). These data demonstrate that interaction between PrpS and PrsS in leaf protoplasts is sufficient to induce cell death in an *S*-specific manner. This provides further evidence that the *S*-determinants can operate ectopically in totipotent protoplasts.

Co-expression of *PrsS* and *PrpS* triggers *S*-specific cell death in whole plants

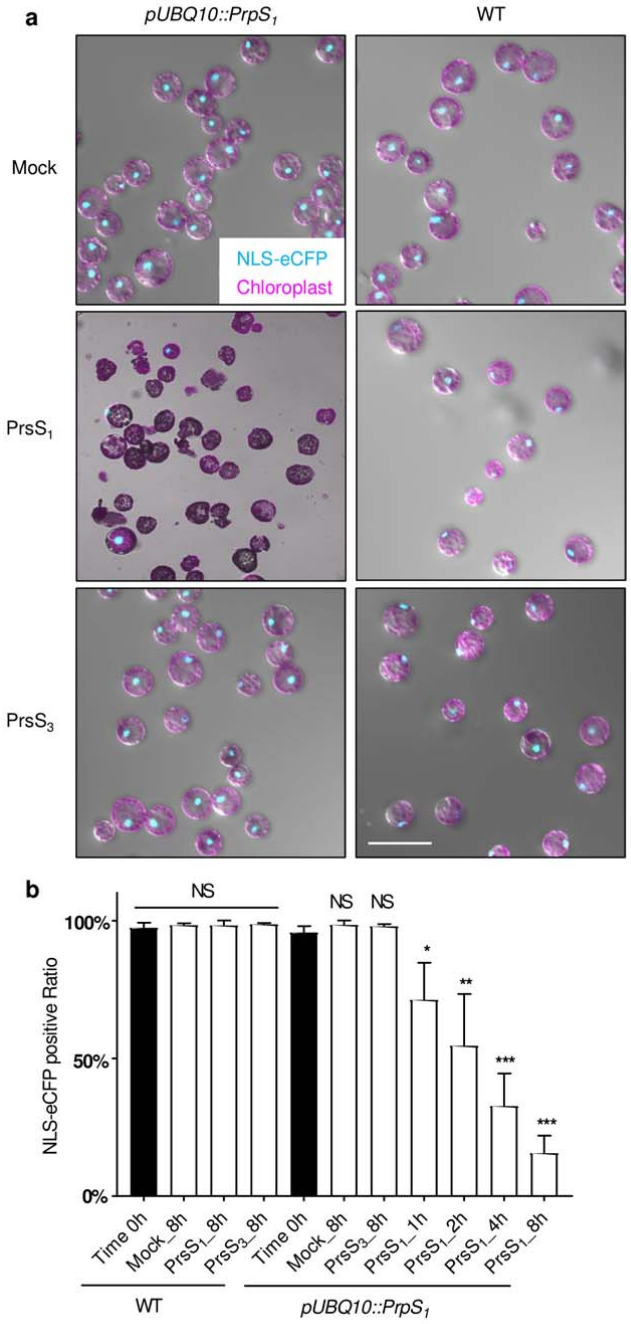

Fig 4. PrpS-expressing leaf protoplasts treated with PrsS undergo *S*-specific cell death.

(a) Representative images of *pUBQ10::PrpS$_1$*/*pUBQ10::NLS-YC3.6* (line 11) leaf protoplasts after PrsS treatment (10 ng.µl^{-1}) for 8h showing bright field images combined with autofluorescent chloroplast signals (magenta) and fluorescent NLS-eCFP signals (turquoise), indicating nuclear integrity. Only *PrpS$_1$*-expressing protoplasts treated with cognate PrsS$_1$ (middle left) showed loss of the nuclear signal, abnormal cell shape and leakage of cellular content. This provides evidence for *S*-specific cell death triggered by cognate PrsS$_1$ in undifferentiated cells. Bar = 100 µm.

(b) Quantification of loss of nuclear integrity in *pUBQ10::PrpS$_1$*/*pUBQ10::NLS-YC3.6* (line 11) leaf protoplasts over time by counting NLS-eCFP signals (turquoise). PrsS$_1$ or PrsS$_3$ treatment (10 ng.µl^{-1}) did not affect the nuclear integrity of WT protoplasts. The percentage of *PrpS$_1$*-expressing protoplasts with a NLS-eCFP signal was significantly reduced by PrsS$_1$ treatment, from ~96% at time 0 h to ~16% at 8h, but no significant difference was observed with PrsS$_3$ after 8 h. Data show mean ± SD; 100-150 cells were counted in each treatment for each timepoint, n=3. One-way ANOVA with multiple comparisons of "time = 0h" with each of the other treatments at each time-point. NS, not significant; *, p<0.05; **, p<0.01; ***, p<0.001.

Finally, we investigated whether PrsS, when expressed *in planta*, was able to exert the same effect as treatment with recombinant PrsS protein in whole plants. We introduced PrsS into the *pUBQ10::PrpS$_1$* background line under the control of an estradiol inducible promoter (*pH3.3::XVE::PrsS$_{1/3}$/pUBQ10::PrpS$_1$*, referred to as *XVE::PrsS$_{1/3}$/PrpS$_1$* hereafter). *XVE::PrsS$_1$/PrpS$_1$* seeds completely failed to germinate on medium containing estradiol. In contrast, no significant difference in the germination rate (95.5% - 97.5%) of the background *pUBQ10::PrpS$_1$* line and *XVE::PrsS$_3$/PrpS$_1$* line was observed before and after estradiol

induction (**Table 1**). This effect on seed germination demonstrated that simultaneous expression of cognate *PrpS* and *PrsS* in seeds induces cell death *in planta*.

To test this hypothesis and examine cell viability after estradiol induction further, we induced $PrsS_{1/3}$ expression by transferring *XVE::*$PrsS_{1/3}$*/*$PrpS_1$ seedlings to medium containing estradiol. Root growth was rapidly inhibited after transfer to estradiol, whereas *pUBQ10::*$PrpS_1$ and *XVE::*$PrsS_3$*/*$PrpS_1$ seedlings were not affected (**Fig 5a, b**; **Fig S10**). Strikingly, the *XVE::*$PrsS_1$*/*$PrpS_1$ seedlings were stunted and cotyledons were white after 48 h on estradiol (**Fig 5a**). These data show that the estradiol-induced expression of $PrsS_1$ (**Fig S11**) is sufficient to cause *S*-specific root growth inhibition and subsequent systemic PCD of the entire *pUBQ10::*$PrpS_1$ seedling. Moreover, time-lapse examination of *XVE::*$PrsS_1$*/*$PrpS_1$ seedling roots expressing NLS-YC3.6 after estradiol treatment revealed localized increases in $[Ca^{2+}]_{nuc}$ 3 h after estradiol induction (**Fig 5c**), providing evidence for estradiol-induced expression of PrsS, and subsequent PrpS-PrsS interaction. At 5 h, a dramatic decrease in nuclear integrity was observed in root tips, and this continued for up to 11 h, when almost no cells with intact nuclei were observed in root tips (**Fig 5c**). PI staining showed that besides the loss of nuclear integrity, plasma membrane permeability was also affected (**Fig 5d**). Thus, cell death triggered by co-expression of cognate PrpS and PrsS was observed in whole root tissues (**Fig S12**). Control plants that expressed non-cognate $PrsS_3$ and $PrpS_1$ exhibited no major changes in nuclear integrity after estradiol induction (**Fig S12**). Together these data demonstrate that the co-expression of cognate *PrpS* and *PrsS* induces the death of the whole plant in Arabidopsis. This suggests that this two-component system is capable of triggering cell death when they are expressed together, regardless of tissue or cell type.

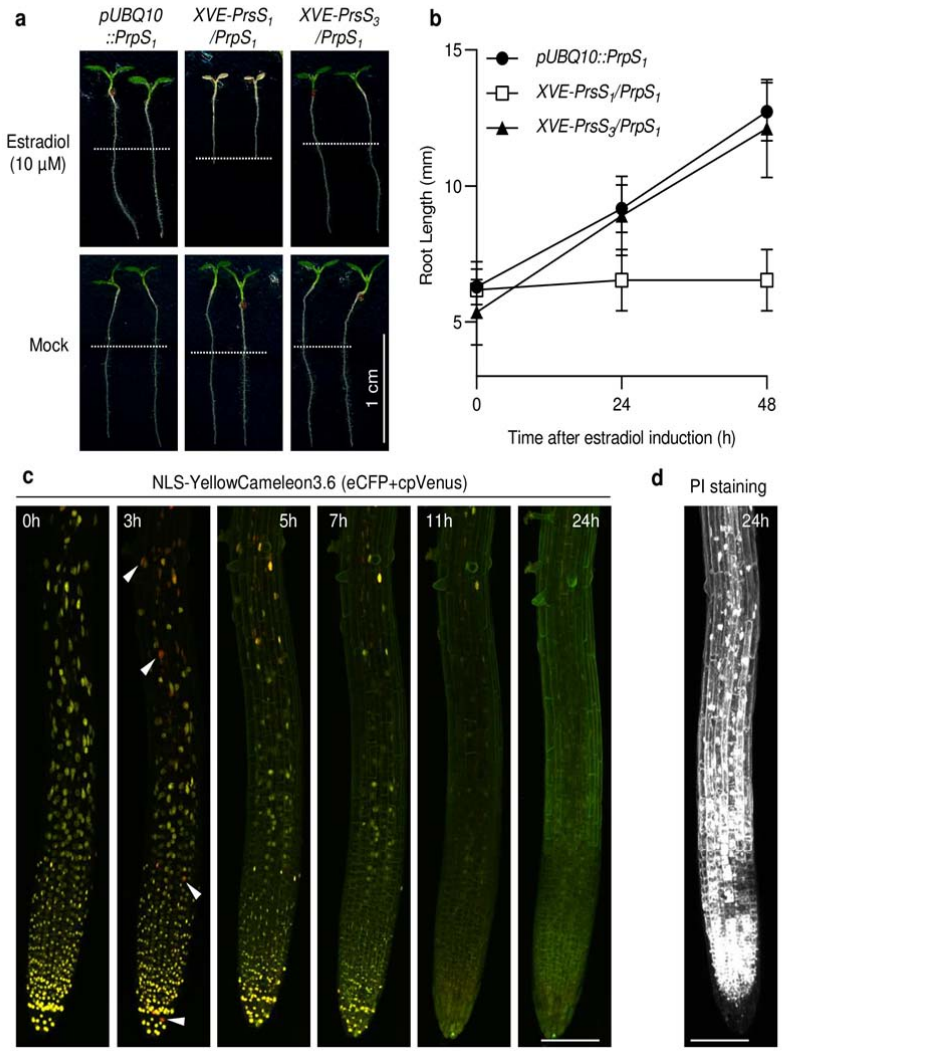

Fig 5. Endogenous expression of PrpS and PrsS in *Arabidopsis thaliana* triggers cell death in whole seedlings in an *S*-specific manner.

(a, b) Root growth of *XVE-PrsS$_1$/PrpS$_1$* seedlings was inhibited after estradiol induction in an *S*-specific manner. (a) 4-day-old seedlings were transferred to new media containing 10 µM estradiol. Images were taken 48h after treatment. White dashed lines indicate the position of the root tips at the time of transfer. Estradiol induced expression of $PrsS_1$ resulted in the death of the whole seedling, whereas no obvious effect was observed when $PrsS_3$ was expressed. (b) Quantification of root length at 24h and 48h after estradiol induction reveals inhibition of root growth in *XVE-PrsS$_1$/PrpS$_1$* lines upon transfer to estradiol plates, whereas the growth of roots of *XVE-PrsS$_3$/PrpS$_1$* and *pUBQ10::PrpS$_1$* seedlings was not affected (mean ± SD, N = 20 seedlings).

(c) Estradiol induction resulted in nuclear disintegration and cell death of *XVE-PrsS$_1$/PrpS$_1$* seedlings. NLS-YC3.6 was used to monitor the nuclear integrity after estradiol induction over time. Confocal images of merged eCFP (LUT colour: green) and cpVENUS (LUT colour: red) channels are shown. The yellow signal (green-red overlap) shows intact nuclei; extensive nuclear disintegration (loss of yellow signal) was observed as early as 5h after estradiol induction and was almost complete by 11 h. The fluorescence signal was so weak at 5h that the confocal laser power was increased from 1.5% (0, 3 h) to 3.5% (5, 7, 11, 24 h) to allow visualization of the seedling. NLS-YC3.6 monitors $[Ca^{2+}]_{nuc}$ and reveals increases (red signal, indicated by white triangles) could be observed 3h after induction. Bar = 100 µm.

(d) PI staining of a representative root at 24h after estradiol induction reveals that virtually all the cells are dead (white signal). Bar = 100 µm.

396 **Discussion**

The *S*-locus in *Papaver* encodes a pair of *S*-determinants, *PrpS* and *PrsS*. Their tissue- and development-specific expression, solely in pollen and pistil respectively, is tightly regulated and they interact in an allele-specific manner to specify and mediate the SI response within the male gametophyte pollen during early pollination. We previously demonstrated functional inter-generic transfer of the *Papaver S*-determinants to the reproductive system of *A. thaliana* (de Graaf et al., 2012; Lin et al., 2015). Here we show that *PrpS* and *PrsS* do not just function as *S*-determinants to specify SI, but that they can operate beyond their usual reproductive context. We demonstrate that the effect of this "self-recognition:self-destruct" mechanism is not confined to the male gametophyte, but *PrpS* and *PrsS* can also act as a heterologous bipartite module to trigger a canonical "SI-like" response resulting in growth inhibition and PCD independent of the reproductive context, when ectopically expressed in sporophytic tissues of *A. thaliana*.

Pollen is a highly specialized gametophytic organism with very specific, precise functions related to reproduction. As such, pollen displays a distinct molecular profile that is distinct from all other plant tissues (da Costa-Nunes and Grossniklaus, 2003; Honys and Twell, 2004; Mergner et al., 2020). The finding here that PrpS and PrsS can act outside of this reproductive context to trigger an "SI-like" growth arrest and PCD response in vegetative cells of the sporophyte when expressed ectopically is surprising, exciting and not predicted by our earlier studies. To our knowledge, ectopic transfer of a two-component module from the reproductive context into the vegetative sporophytic one has not previously been reported in plants. This is a milestone, as it demonstrates that these two genes, which are normally responsible for controlling a reproductive trait, are sufficient to trigger signaling to growth arrest and cell death in numerous cell types, independent of their particular tissue-specific and developmental context.

Our data showing that the *PrpS-PrsS* module can act ectopically provide potential new clues to the possible origin and evolution of bipartite genetic modules that act in cell-cell signaling networks. *PrsS* has homologues in a large family named after them: *S-Protein Homologues* (*SPH*s; also known as *Plant self-incompatibility protein S1 homologs* in the databases), comprising >1800 homologous sequences in >70 plant species as well as in fungi and metazoa (Rajasekar et al., 2019; Ride et al., 1999). Over ninety *SPH*s have been identified in *A. thaliana* (Rajasekar et al., 2019). Based on the large number of *SPH* family members, all encoding proteins with signal peptides, together with their wide distribution, it has previously

been proposed that they may be ligands involved in a wide range of signaling pathways (Ride et al., 1999). It has been suggested that this family of proteins may have evolved to act as a versatile and stable scaffold to display a variety of peptides in the predicted extracellular loops, each interacting with a different receptor (Rajasekar et al., 2019). Our findings here, showing that PrsS can trigger responses in vegetative tissues, provide further hints that (depending on how they have evolved), perhaps other SPHs may be involved in signaling in different tissues.

PrsS and *SPH*s are members of the cysteine-rich peptides (CRPs), which include the Brassica pollen *S*-determinant *SCR/SP11* (Schopfer et al., 1999; Takayama et al., 2000), defensins (Bircheneder and Dresselhaus, 2016), *LUREs* (Okuda et al., 2009; Takeuchi and Higashiyama, 2016) and rapid alkanization factors, *RALFs* (Li and Yang, 2018; Pearce et al., 2001), which are known to interact with receptors to activate diverse signaling networks involved in plant growth, defence and reproduction (Liu et al., 2017; Marshall et al., 2011; Takeuchi and Higashiyama, 2016; Wheeler et al., 2010). Although comparatively few secreted peptides have been shown to interact with receptors in plants, genome analysis has revealed the existence of hundreds of predicted secreted proteins that may act as ligands (Lease and Walker, 2006). It has been suggested that CRPs have diversified for a huge variety of specialized functions (Bircheneder and Dresselhaus, 2016; Manners, 2007; Silverstein et al., 2007); rapid evolution from an origin in plant defence to regulate plant reproduction has been proposed (Bircheneder and Dresselhaus, 2016). Analysis of Arabidopsis *SPH* genes in the available databases reveal that they are mainly, but not exclusively, expressed in reproductive tissues (**Fig S13**, **S14**; (Mergner et al., 2020). Notably, several *SPHs* are expressed in silique septum, silique valves, flower pedicles and senescent leaves, which all undergo PCD in various cellular/developmental contexts (Beers, 1997; Gómez et al., 2014). This hints that this family may have evolved a general function in several diverse tissues to signal to growth and PCD, like we have found for PrsS in the current study. Examination of the literature and databases reveals that no functional data are currently available for any Arabidopsis *SPHs.* Nevertheless, association networks for one of the *SPH* genes *AT1G51250* using STRING analysis (Szklarczyk et al., 2019), for example, reveals associations/putative interactions with several proteins. These include APPB1 and AT4G02250 which are plant pectin methylesterase inhibitor proteins, implicated in mediating growth; RALFL8, RALFL15 and RALFL26 (RALF-like cell signaling peptides), implicated in regulating plant stress, growth, and development; and LCR72, a cysteine rich peptide,

predicted to encode a PR protein, that itself interacts with other defensins. These interactions hint that this SPH homolog may signal to regulate growth and stress response. As both RALFs and PMEIs are broadly expressed (**Fig S15, S16**; (Mergner et al., 2020)), this suggests that some SPH homologs may also potentially interact with these proteins to mediate these responses in various tissues. However, as to our knowledge, no studies to date have identified a function for any *SPH* in another tissue, and as no other partners for *SPHs* have been identified to date, we cannot speculate much further about the possible functions of putative homologs of *SPH*s or their putative interactors, which is currently a "black box". Although *PrpS*, being a small transmembrane protein with no known homologues, is not a receptor in the classic sense, our findings here, showing that the PrpS-PrsS module can act as a "receptor-ligand-like module" outside its usual reproductive context in vegetative tissues, provide a rare example of a specialized bipartite gene module that that can act in a cell-autonomous manner. Thus, our finding that PrpS-PrsS can function in vegetative tissues, together with information on SPH homologs and their possible interactors may provide clues about how the *SPH*s might potentially have co-evolved to function in different cell types; an interesting avenue to be explored in the future.

Although the downstream cellular responses observed here in Arabidopsis roots in response to PrsS are strikingly similar to what was observed in *Papaver* pollen tubes during the SI response (Wang et al., 2019; Wilkins et al., 2014), a key difference is that roots utilize diffuse growth, whereas a pollen tube elongates by tip growth. Diffuse growth is used by most plant cells and is often contrasted to tip growth. However, despite differences in spatial patterning there may be considerable overlap in the regulatory processes involved in these two types of growth (Cosgrove, 2018; Yang, 2008). Our evidence that the *PrpS-PrsS* module can also inhibit diffuse growth and does not apparently distinguish between these two types of growth, supports this concept. Moreover, it is of interest to note that the peptides of several other CRP members function to regulate different types of growth. For example, RALFs are involved in arrest of root growth and development (Blackburn et al., 2020; Haruta et al., 2014; Pearce et al., 2001), LUREs (specifically expressed in synergid cells) act to control directional growth of pollen tubes to the embryo sac (Okuda et al., 2009), SCR/SP11 act as the male *S*-determinant in Brassica to inhibit self pollen (Schopfer et al., 1999; Takayama et al., 2000), and ZmES4, induces pollen tube growth arrest and bursting to release sperm cells during fertilization (Amien et al., 2010); see (Blackburn et al., 2020; Higashiyama and Yang, 2017; Kanaoka and Higashiyama, 2015) for recent reviews. Further studies are needed to

499 determine if there is a common growth arrest mechanism triggered by these different CRP
500 mediated signaling pathways. Moreover, it would be of considerable interest to investigate if
501 PrsS interacts with RALFs as a putative candidate player in the SI signaling pathway in
502 pollen, as they are involved in signaling *via* ROS to inhibit primary root elongation (Haruta et
503 al., 2014) and it has been established that ROS is involved in the SI-PCD response in pollen
504 (Wilkins et al., 2011).
505
506 We previously showed that *PrpS* and *PrsS* could function to mediate SI and PCD in *A.*
507 *thaliana* pollen, despite the fact that this species is self-compatible (de Graaf et al., 2012; Lin
508 et al., 2015). We proposed that the *Papaver* SI system worked in *A. thaliana* pollen because it
509 could recruit existing proteins to form new signaling networks, by "multitasking" of
510 endogenous components that can act in signaling networks that they do not normally operate
511 in, to provide a specific, predictable physiological outcome. This successful transfer between
512 species suggested that the signaling network and cellular targets downstream of PrpS-PrsS
513 interaction might be present in a wide range of angiosperm species (de Graaf et al., 2012) as
514 this was the simplest explanation of why these genes work in such an evolutionarily diverged
515 (>100 m.y. (Bell et al., 2010)) species. However, we did not explore whether this might
516 extend beyond the particular context of pollen involved in the SI response. Here we have
517 extended our studies to show that this pair of genes can also act in other cell types in *A.*
518 *thaliana*. Our findings here, showing that this module can trigger growth arrest and PCD in
519 sporophytic vegetative cells, provide firm evidence for this idea of "plug and play" and
520 extends it, by showing that PrpS-PrsS can also act in an ectopic situation to trigger a
521 signaling network and response that appears to be common and ubiquitously expressed, and
522 not just restricted to pollen. As key components can be harnessed in different cell types to
523 reconstitute key *Papaver* SI-PCD-like phenomena in vegetative cells, it provides hints about
524 the functional diversification and recruitment of pre-existing components and the plasticity of
525 cell signaling downstream of the PrpS-PrsS interaction leading to growth arrest and PCD in
526 plant cells.
527
528 Our study has substantially extended previous studies (de Graaf et al., 2012; Lin et al., 2015)
529 and reveals that the events downstream of *Papaver* PrpS-PrsS interaction can be triggered in
530 different cell types of *A. thaliana*. This lays the foundations for new opportunities to
531 elucidate key mechanisms triggered by cognate PrpS-PrsS interactions. Although the
532 *Papaver* SI system has provided an excellent model system to investigate cell-cell

recognition, intracellular signalling and PCD at a molecular level, the extremely limited genetic resources in this system has provided an obstacle to progress, as certain approaches were not possible. Our findings here suggest that Arabidopsis plants express an "SI-like response" in vegetative tissues with all the key features of *Papaver* SI, opening up new opportunities to genetically dissect the signalling networks involved. Expression of the bipartite PrpS-PrsS module in different tissues has the potential to be applied to devise biochemical or genetic approaches to search for downstream components. Using this system in vegetative tissue or whole plants has the advantage that it overcomes the bottleneck that many reproductive researchers are faced with, i.e. that of limited material; collecting sufficient pollen at the correct developmental stage is laborious, time-consuming and difficult to scale-up. Being able to perform experiments on bulk plant tissue or on whole plants could allow us to identify new genes/proteins involved in the downstream pathway; these could then be examined and validated in pollen to establish if they authentically play a role in the SI response. For example, root growth assays could provide a simple assay for screening large sets of T-DNA mutants or chemical library screening. Biochemical approaches, such as purification of candidate proteins or profiling of PrpS-PrsS induced metabolomic changes using pollen are generally impossible, due to the small amount of tissue available. Using a heterologous expression system to enable a bulk-purification, from leaves or roots for example, of putative proteases with caspase-like activities or actin-binding proteins implicated in the actin remodeling, might be possible. In conclusion, this ectopic Arabidopsis "self-recognition:self-destruct" system will allow us to test new hypotheses about the cellular mechanisms and genetic components involved in the SI-PCD response and tip growth of plant cells in the future.

Materials and Methods

Plant material and growth conditions

A. thaliana Col-0 seeds were gas sterilized, sown out on LRC2 plates (2.15g/L MURASHIGE & SKOOG MEDIUM basal salts Duchefa Biochemie, 0.1g/L MES, pH adjusted to 5.7 with KOH, 1.0% Plant Tissue Culture Agar NEOGEN), and stored in cold room (4°C) for three days before being moved to growth chamber for vertical growth with continuous light emitted by white fluorescent lamps (intensity 120 µmol m^2 s^{-1}), at 22°C. Unless specifically stated, 4-day-old seedlings after being placed in the growth chamber were used for experiments. When necessary, seedlings were transferred to Jiffy pots in soil and

grown under glasshouse conditions under a 16h light/8h dark regime at 22°C. Plants were protected by ARASYSTEM (http://www.arasystem.com/userguide.php) to stop the pollen spreading when flowering and keep the seed stocks pure. Seeds were collected when the plants were completely dry and kept at room temperature (RT) or 4°C for long-term storage.

Cloning and transgenic lines

All the expression vectors were generated using either Gateway cloning (Invitrogen) or Greengate cloning (Lampropoulos et al., 2013). High-fidelity Phusion DNA polymerase (New England BioLabs) was used for all the DNA fragment amplification.

The expression clones pUBQ10::$PrpS_1$ were obtained using Gateway cloning (Invitrogen). $PrpS_1$ gDNA was amplified using primers F-attB1-$PrpS_1$/R-attB2-$PrpS_1$ with gDNA of line BG16 (de Graaf et al., 2012) as template. The resulting PCR fragments were cloned into pDONR221 using BP clonase (Invitrogen) to obtain pEN-L1-$PrpS_1$-L2. The entry vector pEN-L4-pUBQ10-R1 was obtained from PSB Gateway Vector collection (Fendrych et al., 2014). These entry clones were recombined into Gateway destination vectors pB7m24GW (Karimi et al., 2002) using LR Clonase II plus enzyme (Invitrogen) to obtain the expression clone pUBQ10::$PrpS_1$.

The expression clones pH3.3::XVE::$PrsS_{1/3}$ were generated using Gateway cloning (Invitrogen). DNA fragment of H3.3 promoter was amplified using K1H3-F and X1H3-R primers. PCR products were digested using Kpnl and Xhol restriction enzymes followed by DNA gel purification. Plasmid pEN-L4-pRPS5A::XVE-R1 (Huysmans et al., 2018) was digested using the same restriction enzymes, followed by DNA gel electrophoresis. The vector backbone without the RPS5A promoter was cut out and purified. The Kpnl-pH3.3-Xhol DNA fragment was ligated into the linearized vector backbone to generate pEN-L4-pH3.3::XVE-R1. $PrsS_{1/3}$ gDNA was amplified using primer sets F-attB1-$PrsS_{1/3}$/R-attB2-$PrsS_{1/3}$ with plasmid pSLR1::$PrsS_{1/3}$ (Lin et al., 2015) as template. The resulting PCR fragments were cloned into pDONR221 using BP clonase (Invitrogen) to obtain pEN-L1-$PrsS_{1/3}$-L2. These entry clones were recombined into Gateway destination vectors pB7m24GW-FAST-Green using LR Clonase II plus enzyme (Invitrogen) to obtain the expression clone pH3.3::XVE::$PrsS_{1/3}$.

The dual-expression clones pUBQ10::$PrpS_1$_pUBQ10::NLS-YC3.6, pUBQ10::$PrpS_1$_pUBQ10::YC3.6, pUBQ10::$PrpS_1$_pUBQ10::pHGFP and pUBQ10::$PrpS_1$_pUBQ10::LifeAct-mRuby2 were generated using Greengate cloning. Promoter UBQ10 was amplified using primer sets F-A-pUBQ10/R-B-pUBQ10, F-D-pUBQ10/R-E-pUBQ10 with entry vector pEN-L4-pUBQ10-R1 as the template. The resulting PCR fragments were cloned into pJET1.2 using CloneJET PCR Cloning Kit (ThermoFisher) to obtain the entry vectors pEN-A-pUBQ10-B and pEN-D-pUBQ10-E. Similarly, pEN-B-$PrpS_1$-C was generated by cloning of $PrpS_1$ DNA fragment amplified using primers F-B-$PrpS_1$/R-C-$PrpS_1$ into pJET1.2. To create entry vectors for terminator RBCS (tRBCS), NLS-YC3.6, YC3.6 and tMAS, the corresponding DNA fragments were amplified using primer sets F-C-tRBCS/R-D-tRBCS, F-E-NLS/R-F-YC3.6, F-E-YC3.6/R-F-YC3.6 and F-F-tMAS/R-G-tMAS with expression vector pUBQ10::NLS-YC3.6 (Krebs et al., 2012) as template. The resulting PCR fragments were cloned into pJET1.2 to obtain entry vectors pEN-C-tRBCS-D, pEN-E-NLS-YC3.6-F, pEN-E-YC3.6-F and pEN-F-tMAS-G. pEN-E-pHGFP-F and pEN-E-LifeAct-mRuby2-F was generated by cloning of the DNA fragment pHGFP and LifeAct-mRuby2 into pJET1.2, respectively. pHGFP was amplified using primer set F-E-pHGFP/R-F-pHGFP with the genomic DNA of transgenic line pUBQ10::pHGFP (Fendrych et al., 2014) as template. LifeAct-mRuby2 was amplified using primers F-E-LifeAct/R-F-mRuby2 with the genomic DNA of transgenic line pNTP303::LifeAct-mRuby2 as template. These entry clones were cloned into Greengate destination vectors pFAST-RK-AG (Decaestecker et al., 2019) to obtain the dual-expression vectors pUBQ10::$PrpS_1$_pUBQ10::NLS-YC3.6, pUBQ10::$PrpS_1$_pUBQ10::YC3.6, pUBQ10::$PrpS_1$_pUBQ10::pHGFP and pUBQ10::$PrpS_1$_pUBQ10::LifeAct-mRuby2. Detailed primer information can be found in **Supplemental Table S1**.

The expression vectors were transformed into GV3101 *Agrobacterium tumefaciens* competent cells. The floral-dipping method was adopted to stably transform Col-0 Arabidopsis plants as described previously (Fendrych et al., 2014).

T1 transgenic seeds were screened with LRC2 plates with corresponding antibiotics, or using fluorescence stereomicroscope by checking the fluorescence exhibited by the seeds. Lines with a single T-DNA insertion were obtained by selecting 3:1 segregation ratio with T2 seeds. T3 homozygous seeds were used for all the experiments, if not specified.

RNA extraction, cDNA synthesis and RT-PCR

To examine the $PrpS_1$ mRNA expression in the transgenic line, 10 4-day-old seedlings from each line were collected, with WT seedlings as the control. To examine the $PrsS_{1/3}$ mRNA expression in the pH3.3::XVE::$PrsS_{1/3}$/pUBQ10::$PrpS_1$ transgenic line before and after estradiol treatment, 4-day-old seedlings were transferred onto LRC2 plates containing 10 μM estradiol (LRC2 plates containing 0.1% ethanol as a mock treatment control) for 6h before collected for RNA extraction. Total RNA was extracted using RNeasy Mini Kit (Qiagen). cDNA was synthesized using 500ng of total RNA with the iScript cDNA synthesis kit (BioRad) according to the manufacture's instruction. The RT-qPCR was performed with the LightCycler 480 (Roche) using SYBR green, followed by data analysis using qBase. $PrpS_1$ and $PrsS_{1/3}$ mRNA expression were examined using primer sets F-$PrpS_1$-Q/R-$PrpS_1$-Q and F-$PrsS_{1/3}$-Q/R-$PrsS_{1/3}$-Q, respectively, with Actin2 as housekeeping control (F-Actin2-Q/R-Actin2-Q). Detailed primer information can be found in **Supplemental Table S1**.

PrsS protein treatment

Recombinant PrsS proteins were produced as described (Foote et al., 1994), and stored in -70°C. PrsS proteins were dialysed in 1/5 LRC2 liquid medium overnight in 4°C before use. The concentration of PrsS proteins were determined using Bradford assay (BioRad), during which the standard curve was generated using BSA (Sigma Aldrich). To examine the effect of PrsS proteins on seedling growth, 10 μl PrsS proteins with desired concentration (the PrsS protein concentration used in all the experiments was 10 $ng.\mu l^{-1}$, unless specified) needed for different experiments were added to the root tip of each seedling using pipette on LRC2 plates. The plates were kept horizontally for 30 min to allow the PrsS proteins to dry before being placed back to the growth chamber vertically. When the PrsS protein treatment was needed during live-cell imaging, a perfusion chamber system was adopted. Samples were mounted and treated as described (Krebs and Schumacher, 2013) with minor modifications: instead of cotton, glass wool was used, and half strength MS solution was replaced with 1/5 LRC2 solution. The procedure and concentration of PrsS proteins we used here was similar to what was used to induce the SI-PCD response in pollen growing *in vitro* (de Graaf et al., 2012; Wilkins et al., 2015), apart from the composition of the medium, where, instead of liquid pollen germination medium, 1/5 LRC2 liquid medium was used here.

Protoplast preparation

Leaves from 4-week-old plants were harvested and the lower epidermis was removed using double side tape as described (Wu et al., 2009). These leaf samples were immediately transferred into a petri dish containing protoplast enzymes (1% cellulose R10 Yakult, 0.25% macerozyme R10 Yakult) in protoplast washing solution (0.4 M mannitol, 10 mM $CaCl_2$, 20 mM KCl, 0.1% BSA, 20 mM MES and pH 5.7 adjusted using KOH). Samples were incubated at RT with light on an orbital shaker set to 40 rpm for up to 2 h, followed by gentle filtration using a 70 μm cell strainer into a 50 ml tube. Protoplasts were washed three times with the protoplast washing solution by centrifuging at 100g for 3 min and aspirate off the supernatant, followed by suspension in protoplast washing solution, before being subject to PrsS treatment. PrsS proteins used for protoplast treatment were dialysed in protoplast washing solution without BSA overnight in 4°C. BSA was added back to the protoplast washing solution after PrsS protein concentration determination using Bradford assay (BioRad). PrsS proteins treatment for protoplast was carried out in 12-well tissue culture plate. PrsS proteins were added to the protoplast directly to a final concentration 10 $ng.\mu l^{-1}$. Protoplast washing solution was added as mock control. During treatments, plates were placed at Arabidopsis growth chamber with continuous light emitted by white fluorescent lamps (intensity 120 $\mu mol\ m^2\ s^{-1}$), at 22°C. Fifty μl of protoplast samples were taken out from the plate at 0h (before treatment), 1h, 2h, 4h and 8h respectively for viability examination and confocal imaging.

Estradiol induction

B-estradiol (Sigma-Aldrich) was dissolved in pure ethanol, and 10 mM stock solution was prepared. Stock solution was stored in -20°C for up to 1 month. Four-day-old seedlings grown on LRC2 plates were transferred onto LRC2 plates containing estradiol (10 μM) or 0.1% ethanol (mock control) for a specified period of time according to different experiments.

DEVDase activity assay

CV-Caspase3&7 detection Kit (Enzo Life Science) was used for measuring the DEVDase activities of seedlings after PrsS proteins treatment. DEVDase activity probe $CR(DEVD)_2$ powder was reconstituted using 100 μl DMSO to obtain $CR(DEVD)_2$ stock solution and kept in -20°C if not utilized immediately. Before use, the stock solution was diluted 1:5 in MilliQ water to make the staining solution. The working solution was made by further diluting the

staining solution 1:20 in 1/5 LRC2 solution. Samples were incubated in the working solution for 1h at RT before imaging.

Imaging, image analysis and figure preparation

Imaging of the root calcium signature was performed using a Zeiss LSM710 microscope using a PlanApochromat 20x objective (numerical aperture 0.8). YC3.6 or NLS-YC3.6 was excited with 405 nm and fluorescence emissions 460-515 nm and 515-570 nm were collected for ECFP and cpYenus, respectively. When propidium iodide (PI) staining was perform in conjunction with NLS-YC3.6 signal acquisition, seedling samples were mounted with 1/5 LRC2 medium containing 5 $\mu g.ml^{-1}$ PI. A new imaging track was set up for PI signal acquisition. PI was excited with 561 nm and fluorescence emission between 580 nm and 700 nm were collected.

Imaging of the root pHGFP signal was performed using a Zeiss LSM710 microscope using a PlanApochromat 20x objective (numerical aperture 0.8). PHGFP was excited with 405 nm and 488 nm, respecitively, and fluorescence emissions between 495 nm and 545 nm were collected.

LifeAct visualization was acquired using a Leica SP8 confocal laser scanning system with HCPL APO CS2 40x/1.10 (water) objective and HyD detector. LifeAct-mRuby2 was excited with 559 nm and fluorescence emissions between 570 nm and 700 nm were collected.

DEVDase activities were visualized using a Leica SP8 confocal laser scanning system with Fluostar VISIR 25x/0.95 (water) objective and HyD detector. Samples were excited with 592 nm, and fluorescence emissions between 610nm and 690 nm were collected.

All the images were processed and analysed using Fiji (https://fiji.sc/). To quantify the calcium signal from NLS-YC3.6 or YC3.6 images, fluorescent intensities of the selected regions of interest (ROIs) were extracted using Fiji for both the eCFP and cpVenus channels. Fractional ratio changes ($\Delta R/R$) were calculated as (R-R0)/R0, where R0 is the average ratio of the first 5 min (15 frames) of each measurement.

Statistical analysis

Statistical analysis was performed using GraphPad Prism 8.0 for Windows (www.graphpad.com).

Accession Numbers

Sequence data from this article can be found in the GenBank/EMBL data libraries under accession numbers:_Actin2 (At3g18780); UBQ10 (At4g05320); H3.3 (At4g40040).

List of Supplemental Data

Supplemental Figure S1. RT-qPCR shows that expression of *PrpS$_1$* mRNA varies in different *pUBQ10::PrpS$_1$* lines.

Supplemental Figure S2. Treatment with PrsS$_1$ proteins does not inhibit the growth of wild type (WT) seedlings.

Supplemental Figure S3. Recombinant PrsS protein treatment triggers rapid root growth inhibition of *PrpS*-expressing seedlings in an *S*-specific manner.

Supplemental Figure S4. PrsS treatment results in *S*-specific cell death of *PrpS*-expressing seedling root cells.

Supplemental Figure S5. PrsS treatment results in *S*-specific activation of DEVDase in *PrpS*-expressing seedling roots.

Supplemental Figure S6. PrsS treatment triggers *S*-specific alterations in $[Ca^{2+}]_{cyt}$

Supplemental Figure S7. PrsS treatment triggers nuclear-localized Ca^{2+} changes in an *S*-specific manner.

Supplemental Figure S8. PrsS treatment triggers *S*-specific cytosolic pH decreases in *PrpS*-expressing roots.

Supplemental Figure S9. PrsS treatment triggers *S*-specific formation of actin foci in *PrpS*-expressing roots.

Supplemental Figure S10. Co-expression of PrpS and PrsS in *Arabidopsis thaliana* triggers root growth inhibition in an *S*-specific manner.

Supplemental Figure S11. Estradiol treatment induces the expression of *PrsS* mRNA transcript in *XVE-PrsS/PrpS$_1$* lines.

Supplemental Figure S12. Co-expression of PrpS and PrsS in whole *Arabidopsis thaliana* plants using estradiol triggers *S*-specific cell death in whole seedling roots.

Supplemental Figure S13. Transcript expression patterns of the *S Protein Homologue* (*SPH*) genes in *Arabidopsis thaliana* tissues.

Supplemental Figure S14. Protein expression patterns of the *S Protein Homologue* (*SPH*) genes in *Arabidopsis thaliana* tissues.

Supplemental Figure S15. Expression patterns of Rapid Alkalinization Factors (RALFs) in *Arabidopsis thaliana* tissues.

Supplemental Figure S16. Expression patterns of Pectin Methylesterase Inhibitors (PMEIs) in *Arabidopsis thaliana* tissues.

Supplemental Table S1. Primers for vector construction and mRNA detection.

Acknowledgments

We thank members of the PCD laboratory for critical comments on the manuscript, Dr. Melanie Krebs (University of Heidelberg) for sharing YC3.6-related vectors and seeds, and Dr. Rafael Andrade Buono (Gent University) for providing the root image for Figure 2a. We gratefully acknowledge funding by the ERC StG PROCELLDEATH (Project Number: 749 639234) to MKN, and the Biotechnology, Biological Sciences Research Council (grant numbers BB/P005489/1) to VEF-T and MB, and funding by the FWO (project numbers G011215N and 12I7417N) to MT and ZL, respectively. FX is funded by Chinese Scholarship Council (201806760049).

TABLES

Table 1. Co-expression of cognate *PrsS* and *PrpS* completely abolishes *Arabidopsis thaliana* seed germination

Treatment	*pUBQ10::PrpS$_1$*	*XVE-PrsS$_1$/PrpS$_1$*	*XVE-PrsS$_3$/PrpS$_1$*
Mock	95.5% (128/134)	96.1% (147/153)	97.5% (197/202)
Estradiol	96.6% (113/117)	0.0% (0/108)	97.0% (131/135)

Newly harvested seeds of different lines were sown on LRC2 plates containing estradiol (10 µM) or solvent (ethanol, mock control), and germination rate was recorded 4 days after being placed into a growth chamber. The numbers between brackets indicate the number of

809 germinated seeds/the total number of seeds being examined. After mock treatment, the seed
810 germination rates of the lines *pUBQ10::PrpS$_1$*, *XVE-PrsS$_1$/PrpS$_1$* and *XVE-PrsS$_3$/PrpS$_1$* are
811 comparable to each other (~95-97%). Estradiol induction does not affect the germination rate
812 of *pUBQ10::PrpS$_1$*, nor *XVE-PrsS$_3$/PrpS$_1$*, whereas induced expression of $PrsS_1$ completely
813 abolishes *XVE-PrsS$_1$/PrpS$_1$* germination.
814
815
816

FIGURE LEGENDS

Fig 1. Expression of *PrpS* in transgenic *Arabidopsis thaliana* triggers root growth inhibition after cognate PrsS treatment.

(a) RT-PCR shows the expression of $PrpS_1$ mRNA in $pUBQ10::PrpS_1$ transgenic seedlings. *Actin2* was used as a housekeeping gene control. Quantification of the relative expression levels is shown in Fig S1.

(b, c) *S*-specific inhibition of root growth of $pUBQ10::PrpS_1$ seedlings after $PrsS_1$ treatment.

(**b**) Images of 4-day-old seedlings 24 h after treatment with PrsS proteins (10 ng.μl^{-1}). Black lines indicate the position of root tips when treated. Only $pUBQ10::PrpS_1$ seedlings (line 12) treated with $PrsS_1$ (bottom, centre) display inhibited root growth. This line was used for all the other experiments if not specified. Bar = 1 cm.

(**c**) Quantitation of increases in seedling root length from different transgenic lines (see (a)) treated with PrsS proteins (10 ng. μl^{-1}) 24h after treatment (mean ± SD, n = 20-25 seedlings). All five lines had root growth significantly inhibited by $PrsS_1$ when comparisons were made with either $PrsS_3$ or "mock" treatment for each line (Two-way ANOVA multiple comparison; NS, not significant; ***, $p<0.001$).

(d) Root growth of $pUBQ10::PrpS_1$ seedlings was inhibited by $PrsS_1$ in a dose-dependent manner. X-axis indicates time (days) after transferal of plates to the growth chamber. Arrow indicates when the treatment was added. Result = mean ± SD, n = 20-25 seedlings.

(e) $PrsS_1$ treatment induces rapid root growth inhibition of $pUBQ10::PrpS_1$ seedlings in an *S*-specific manner. Arrow indicates the time-point of PrsS addition (10 ng. μl^{-1}). Two-way ANOVA shows $PrsS_1$ treatment significantly inhibited root growth ($p<0.001$, ***), while $PrsS_3$ did not ($p=0.29$), in comparison with WT seedlings treated with $PrsS_1$. Result = mean ± SD, n = 6.

Fig 2. PrsS treatment results in cell death of *PrpS*-expressing seedling root cells.

(a) An image of a root illustrating different regions of the root tip. Cell files of epidermis, cortex and endodermis are indicated by blue, red and black stars, respectively.

(b) PrsS treatment results in the *S*-specific cell death of $pUBQ10::PrpS_1$ roots. Representative images of $pUBQ10::PrpS_1$ roots expressing NLS-YC3.6 stained with PI 24h after treatment (n>6). No death was observed in roots mock-treated with buffer (mock), as shown by the absence of PI staining (PI, left hand images). Cognate $PrsS_1$ treatment (10 ng.

851 µl^{-1}) resulted in high levels of PI staining (white) in *pUBQ10::PrpS$_1$* seedling roots, but those
852 treated with compatible PrsS$_3$ (10 ng. µl^{-1}) did not. The NLS-cpVENUS signal (yellow) also
853 reveals evidence of cell death, as it is lost after cognate PrsS$_1$ addition. Images were taken
854 24h after treatment. Bar = 100 µm.
855 **(c) PrsS treatment activates a DEVDase activity in *pUBQ10::PrpS$_1$* seedling roots.**
856 DEVDase activity was monitored using the CR(DEVD)$_2$ probe (purple). Besides endogenous
857 DEVDase activity detected in the lateral root cap (indicated by white triangles), no DEVDase
858 activity was observed in the root tip of WT seedlings before or after PrsS$_1$ (10 ng. µl^{-1})
859 treatment. For the *PrpS$_1$*-expressing root, DEVDase activity was observed within 1 h of PrsS$_1$
860 addition in different cell types including epidermis, cortex and endodermis, of both the
861 meristem and elongation zone of the root tip, and activity subsequently increased further.
862 Representative images (n=5) of single Z-optical sections are shown here; a full projection
863 image is shown in Fig S5. Bar = 100 µm.
864
865 **Fig 3. Key hallmarks of *Papaver* SI response are observed in the *Arabidopsis thaliana***
866 ***PrpS*-expressing roots after PrsS treatment.**
867 **(a) PrsS induces transient increases in cytosolic free Ca^{2+} ([Ca^{2+}]$_{cyt}$) in cognate *PrpS*-**
868 **expressing Arabidopsis seedling roots.** Quantitation of changes in [Ca^{2+}]$_{cyt}$ measured in
869 Arabidopsis seedling roots in the elongation zone (left hand image ROI, dotted box), using
870 the Ca^{2+} marker YC3.6 signal expressed as fractional ratio changes (ΔR/R0; mean ± SD,
871 n=6). After PrsS addition (10 ng. µl^{-1}, indicated by arrow) an increase in [Ca^{2+}]$_{cyt}$ was
872 observed in in the elongation zone of *pUBQ10::PrpS$_1$* roots treated with PrsS$_1$ (magenta);
873 controls (black, blue) did not display this response.
874 **(b, c) PrsS triggers acidification in cognate *PrpS*-expressing Arabidopsis seedling root.**
875 (b) Ratiometric (405nm/488nm) imaging of *pUBQ10::PrpS$_1$* roots expressing the pH sensor
876 pHluorin after PrsS$_1$ (10 ng. µl^{-1}) addition revealed that the signal ratio decreased, indicating
877 cytosolic acidification. Bar = 100 µm. (c) Quantification of the pHluorin ratio measured in
878 the ROI (white dotted box in (b)) of these roots shows a significant decrease in [pH]$_{cyt}$ after
879 SI induction (mean ± SD, n=12; one-way ANOVA with multiple comparison test, between a
880 & b, b & c: $p<0.001$; c *vs* c is N.S.). The pHluorin ratio at time = 0 h was normalized to 1.
881 **(d) PrsS treatment triggers *S*-specific loss of actin filaments and formation of actin foci**
882 **in roots.**
883 Representative images (n>6) of confocal imaging of *pUBQ10::PrpS$_1$* roots (elongation zone)
884 expressing LifeAct-mRuby2. (i) Prior to treatment, typical longitudinal actin filament

bundles were observed. (ii) 3 h after treatment with $PrsS_1$ (10 ng. μl^{-1}) actin foci were observed (magenta dotted box and magnification of this region to the right). (iii) The same line at 3 h after addition of $PrsS_3$ proteins (10 ng. μl^{-1}) displayed normal longitudinal actin filament bundles. Images are full projections, white bars = 50 µm, magenta bar = 10 µm.

Fig 4. PrpS-expressing leaf protoplasts treated with PrsS undergo *S*-specific cell death.
(a) Representative images of *pUBQ10::PrpS$_1$/pUBQ10::NLS-YC3.6* (line 11) leaf protoplasts after PrsS treatment (10 ng. μl^{-1}) for 8h showing bright field images combined with autofluorescent chloroplast signals (magenta) and fluorescent NLS-eCFP signals (turquoise), indicating nuclear integrity. Only *PrpS$_1$*-expressing protoplasts treated with cognate $PrsS_1$ (middle left) showed loss of the nuclear signal, abnormal cell shape and leakage of cellular content. This provides evidence for *S*-specific cell death triggered by cognate $PrsS_1$ in undifferentiated cells. Bar = 100 µm.
(b) Quantification of loss of nuclear integrity in *pUBQ10::PrpS$_1$/pUBQ10::NLS-YC3.6* (line 11) leaf protoplasts over time by counting NLS-eCFP signals (turquoise). $PrsS_1$ or $PrsS_3$ treatment (10 ng. μl^{-1}) did not affect the nuclear integrity of WT protoplasts. The percentage of *PrpS$_1$*-expressing protoplasts with an NLS-eCFP signal was significantly reduced by $PrsS_1$ treatment, from ~96% at time 0 h to ~16% at 8h, but no significant difference was observed with $PrsS_3$ after 8 h. Data show mean ± SD; 100-150 cells were counted in each treatment for each timepoint, n=3 experiments. One-way ANOVA with multiple comparisons of "time = 0h" with each of the other treatments at each time-point. NS, not significant; *, $p<0.05$; **, $p<0.01$; ***, $p<0.001$.

Fig 5. Ectopic expression of PrpS and PrsS in *Arabidopsis thaliana* triggers cell death in whole seedlings in an *S*-specific manner.
(a, b) Root growth of *XVE-PrsS$_1$/PrpS$_1$* seedlings was inhibited after estradiol induction in an *S*-specific manner. (a) 4-day-old seedlings were transferred to new media containing 10 µM estradiol. Images were taken 48h after treatment. White dashed lines indicate the position of the root tips at the time of transfer. Estradiol induced expression of $PrsS_1$ resulted in the death of the whole seedling (top, centre), whereas no obvious effect was observed when $PrsS_3$ was expressed (top, right). (b) Quantification of root length at 24h and 48h after estradiol induction reveals inhibition of root growth in *XVE-PrsS$_1$/PrpS$_1$* lines upon transfer to estradiol plates, whereas the growth of roots of *XVE-PrsS$_3$/PrpS$_1$* and *pUBQ10::PrpS$_1$* seedlings was not affected (mean ± SD, n = 20 seedlings).

(c) Estradiol induction resulted in nuclear disintegration and cell death of *XVE-PrsS$_1$/PrpS$_1$* seedlings. NLS-YC3.6 was used to monitor the nuclear integrity after estradiol induction over time. Confocal images of merged eCFP (LUT colour: green) and cpVENUS (LUT colour: red) channels are shown. The yellow signal (green-red overlap) shows intact nuclei; extensive nuclear disintegration (loss of yellow signal) was observed as early as 5h after estradiol induction and was almost complete by 11 h. The fluorescence signal was so weak at 5h that the confocal laser power was increased from 1.5% (0, 3 h) to 3.5% (5, 7, 11, 24 h) to allow visualization of the seedling. NLS-YC3.6 monitors $[Ca^{2+}]_{nuc}$ and reveals increases (red signal, indicated by white triangles) could be observed 3h after induction. Bar = 100 μm.

(d) PI staining of a representative root at 24h after estradiol induction reveals that virtually all the cells are dead (white signal). Bar = 100 μm.

934

Parsed Citations

Amien, S., Kliwer, I., Márton, M.L., Debener, T., Geiger, D., Becker, D., and Dresselhaus, T. (2010). Defensin-like ZmES4 mediates pollen tube burst in maize via opening of the potassium channel KZM1. PLoS biology 8, e1000388-e1000388.
Pubmed: Author and Title
Google Scholar: Author Only Title Only Author and Title

Bascom, C.S., Winship, L.J., and Bezanilla, M. (2018). Simultaneous imaging and functional studies reveal a tight correlation between calcium and actin networks. Proceedings of the National Academy of Sciences 115, E2869-E2878.
Pubmed: Author and Title
Google Scholar: Author Only Title Only Author and Title

Beers, E.P. (1997). Programmed cell death during plant growth and development. Cell death and differentiation 4, 649-661.
Pubmed: Author and Title
Google Scholar: Author Only Title Only Author and Title

Bell, C.D., Soltis, D.E., and Soltis, P.S. (2010). The age and diversification of the angiosperms re-revisited. American Journal of Botany 97, 1296-1303.
Pubmed: Author and Title
Google Scholar: Author Only Title Only Author and Title

Bircheneder, S., and Dresselhaus, T. (2016). Why cellular communication during plant reproduction is particularly mediated by CRP signalling. Journal of Experimental Botany 67, 4849-4861.
Pubmed: Author and Title
Google Scholar: Author Only Title Only Author and Title

Blackburn, M.R., Haruta, M., and Moura, D.S. (2020). Twenty Years of Progress in Physiological and Biochemical Investigation of RALF Peptides. Plant Physiol 182, 1657-1666.
Pubmed: Author and Title
Google Scholar: Author Only Title Only Author and Title

Bosch, M., and Franklin-Tong, V.E. (2007). Temporal and spatial activation of caspase-like enzymes induced by self-incompatibility in Papaver pollen. Proceedings of the National Academy of Sciences (USA) 104, 18327-18332.
Pubmed: Author and Title
Google Scholar: Author Only Title Only Author and Title

Boutilier, K., Offringa, R., Sharma, V.K., Kieft, H., Ouellet, T., Zhang, L., Hattori, J., Liu, C.-M., van Lammeren, A.A.M., Miki, B.L.A., et al. (2002). Ectopic Expression of BABY BOOM Triggers a Conversion from Vegetative to Embryonic Growth. The Plant Cell 14, 1737-1749.
Pubmed: Author and Title
Google Scholar: Author Only Title Only Author and Title

Breiden, M., and Simon, R. (2016). Q&A: How does peptide signaling direct plant development? BMC Biology 14, 58.
Pubmed: Author and Title
Google Scholar: Author Only Title Only Author and Title

Cosgrove, D.J. (2018). Diffuse Growth of Plant Cell Walls. Plant Physiol 176, 16-27.
Pubmed: Author and Title
Google Scholar: Author Only Title Only Author and Title

da Costa-Nunes, J.A., and Grossniklaus, U. (2003). Unveiling the gene-expression profile of pollen. Genome Biol 5, 205-205.
Pubmed: Author and Title
Google Scholar: Author Only Title Only Author and Title

de Graaf, B H.J., Vatovec, S., Juárez-Díaz, J A., Chai, L., Kooblall, K., Wilkins, K., Zou, H., Forbes, T., Franklin, F.C H., and Franklin-Tong, V E. (2012). The Papaver Self-Incompatibility pollen S-determinant, PrpS, functions in Arabidopsis thaliana. Current Biology 22, 154-159.
Pubmed: Author and Title
Google Scholar: Author Only Title Only Author and Title

Decaestecker, W., Andrade Buono, R., Pfeiffer, M., Vangheluwe, N., Jourquin, J., Karimi, M., van Isterdael, G., Beeckman, T., Nowack, M.K., and Jacobs, T.B. (2019). CRISPR-TSKO: A Technique for Efficient Mutagenesis in Specific Cell Types, Tissues, or Organs in Arabidopsis. The Plant Cell, tpc.00454.02019.
Pubmed: Author and Title
Google Scholar: Author Only Title Only Author and Title

Diener, A., and Hirschi, K. (2000). Heterologous expression for dominant-like gene activity. Trends in Plant Science 5, 10-11.
Pubmed: Author and Title
Google Scholar: Author Only Title Only Author and Title

Dyachok, J., Sparks, J.A., Liao, F., Wang, Y.S., and Blancaflor, E.B. (2014). Fluorescent protein-based reporters of the actin cytoskeleton in living plant cells: fluorophore variant, actin binding domain, and promoter considerations. Cytoskeleton (Hoboken) 71, 311-327.
Pubmed: Author and Title
Google Scholar: Author Only Title Only Author and Title

Fendrych, M., Van Hautegem, T., Van Durme, M., Olvera-Carrillo, Y., Huysmans, M., Karimi, M., Lippens, S., Guérin, Christopher J., Krebs, M., Schumacher, K., et al. (2014). Programmed Cell Death Controlled by ANAC033/SOMBRERO Determines Root Cap Organ Size in Arabidopsis. Current Biology 24, 931-940.
Pubmed: Author and Title
Google Scholar: Author Only Title Only Author and Title

Fletcher, J.C., Brand, U., Running, M.P., Simon, R., and Meyerowitz, E.M. (1999). Signaling of Cell Fate Decisions by *CLAVATA3* in *Arabidopsis* Shoot Meristems. Science 283, 1911-1914.
Pubmed: Author and Title
Google Scholar: Author Only Title Only Author and Title

Foote, H.C.C., Ride, J.P., Franklin-Tong, V.E., Walker, E.A., Lawrence, M.J., and Franklin, F.C.H. (1994). Cloning and expression of a distinctive class of self-incompatibility (S) gene from Papaver rhoeas L. Proceedings of the National Academy of Sciences (USA) 91, 2265-2269.
Pubmed: Author and Title
Google Scholar: Author Only Title Only Author and Title

Franklin-Tong, V.E., Hackett, G., and Hepler, P.K. (1997). Ratio-imaging of Ca2+ in the self-incompatibility response in pollen tubes of Papaver rhoeas. The Plant Journal 12, 1375-1386.
Pubmed: Author and Title
Google Scholar: Author Only Title Only Author and Title

Franklin-Tong, V.E., Ride, J.P., and Franklin, F.C.H. (1995). Recombinant stigmatic self-incompatibility (S-) protein elicits a Ca2+ transient in pollen of Papaver rhoeas. The Plant Journal 8, 299-307.
Pubmed: Author and Title
Google Scholar: Author Only Title Only Author and Title

Franklin-Tong, V.E., Ride, J.P., Read, N.D., Trewavas, A.J., and Franklin, F.C.H. (1993). The self-incompatibility response in Papaver rhoeas is mediated by cytosolic-free calcium. The Plant Journal 4, 163-177.
Pubmed: Author and Title
Google Scholar: Author Only Title Only Author and Title

Geitmann, A., Snowman, B.N., Emons, A.M.C., and Franklin-Tong, V.E. (2000). Alterations in the actin cytoskeleton of pollen tubes are induced by the self-incompatibility reaction in Papaver rhoeas. Plant Cell 12, 1239-1251.
Pubmed: Author and Title
Google Scholar: Author Only Title Only Author and Title

Gómez, M.D., Vera-Sirera, F., and Pérez-Amador, M.A. (2014). Molecular programme of senescence in dry and fleshy fruits. Journal of Experimental Botany 65, 4515-4526.
Pubmed: Author and Title
Google Scholar: Author Only Title Only Author and Title

Haruta, M., Sabat, G., Stecker, K., Minkoff, B.B., and Sussman, M.R. (2014). A Peptide Hormone and Its Receptor Protein Kinase Regulate Plant Cell Expansion. Science 343, 408-411.
Pubmed: Author and Title
Google Scholar: Author Only Title Only Author and Title

Higashiyama, T., and Yang, W.-C. (2017). Gametophytic Pollen Tube Guidance: Attractant Peptides, Gametic Controls, and Receptors. Plant Physiol 173, 112-121.
Pubmed: Author and Title
Google Scholar: Author Only Title Only Author and Title

Honys, D., and Twell, D. (2004). Transcriptome analysis of haploid male gametophyte development in Arabidopsis. Genome Biol 5, R85-R85.
Pubmed: Author and Title
Google Scholar: Author Only Title Only Author and Title

Huysmans, M., Buono, R.A., Skorzinski, N., Radio, M.C., De Winter, F., Parizot, B., Mertens, J., Karimi, M., Fendrych, M., and Nowack, M.K. (2018). NAC Transcription Factors ANAC087 and ANAC046 Control Distinct Aspects of Programmed Cell Death in the Arabidopsis Columella and Lateral Root Cap. The Plant Cell 30, 2197-2213.
Pubmed: Author and Title
Google Scholar: Author Only Title Only Author and Title

Kanaoka, M.M., and Higashiyama, T. (2015). Peptide signaling in pollen tube guidance. Current Opinion in Plant Biology 28, 127-136.
Pubmed: Author and Title
Google Scholar: Author Only Title Only Author and Title

Karimi, M., Inzé, D., and Depicker, A. (2002). GATEWAY™ vectors for Agrobacterium-mediated plant transformation. Trends in Plant Science 7, 193-195.
Pubmed: Author and Title
Google Scholar: Author Only Title Only Author and Title

Krebs, M., Held, K., Binder, A., Hashimoto, K., Den Herder, G., Parniske, M., Kudla, J., and Schumacher, K. (2012). FRET-based genetically encoded sensors allow high-resolution live cell imaging of Ca2+ dynamics. The Plant Journal 69, 181-192.

Pubmed: Author and Title
Google Scholar: Author Only Title Only Author and Title

Krebs, M., and Schumacher, K. (2013). Live Cell Imaging of Cytoplasmic and Nuclear Ca2+ Dynamics in Arabidopsis Roots. Cold Spring Harbor Protocols 2013, pdb.prot073031.
Pubmed: Author and Title
Google Scholar: Author Only Title Only Author and Title

Lampropoulos, A., Sutikovic, Z., Wenzl, C., Maegele, I., Lohmann, J.U., and Forner, J. (2013). GreenGate - A Novel, Versatile, and Efficient Cloning System for Plant Transgenesis. PLOS ONE 8, e83043.
Pubmed: Author and Title
Google Scholar: Author Only Title Only Author and Title

Lease, K.A., and Walker, J.C. (2006). The Arabidopsis Unannotated Secreted Peptide Database, a Resource for Plant Peptidomics. Plant Physiol 142, 831-838.
Pubmed: Author and Title
Google Scholar: Author Only Title Only Author and Title

Li, H.-J., and Yang, W.-C. (2018). Ligands Switch Model for Pollen-Tube Integrity and Burst. Trends in Plant Science 23, 369-372.
Pubmed: Author and Title
Google Scholar: Author Only Title Only Author and Title

Lin, Z., Eaves, D.J., Sanchez-Moran, E., Franklin, F.C.H., and Franklin-Tong, V.E. (2015). The Papaver rhoeas determinants confer self-incompatibility to Arabidopsis thaliana in planta. Science 350, 684-687.
Pubmed: Author and Title
Google Scholar: Author Only Title Only Author and Title

Liu, X., Zhang, H., Jiao, H., Li, L., Qiao, X., Fabrice, M.R., Wu, J., and Zhang, S. (2017). Expansion and evolutionary patterns of cysteine-rich peptides in plants. BMC Genomics 18, 610-610.
Pubmed: Author and Title
Google Scholar: Author Only Title Only Author and Title

Manners, J.M. (2007). Hidden weapons of microbial destruction in plant genomes. Genome biology 8, 225-225.
Pubmed: Author and Title
Google Scholar: Author Only Title Only Author and Title

Mariani, C., Beuckeleer, M.D., Truettner, J., Leemans, J., and Goldberg, R.B. (1990). Induction of male sterility in plants by a chimaeric ribonuclease gene. Nature 347, 737-741.
Pubmed: Author and Title
Google Scholar: Author Only Title Only Author and Title

Marshall, E., Costa, L.M., and Gutierrez-Marcos, J. (2011). Cysteine-Rich Peptides (CRPs) mediate diverse aspects of cell–cell communication in plant reproduction and development. Journal of Experimental Botany 62, 1677-1686.
Pubmed: Author and Title
Google Scholar: Author Only Title Only Author and Title

Mergner, J., Frejno, M., List, M., Papacek, M., Chen, X., Chaudhary, A., Samaras, P., Richter, S., Shikata, H., Messerer, M., et al. (2020). Mass-spectrometry-based draft of the Arabidopsis proteome. Nature 579, 409-414.
Pubmed: Author and Title
Google Scholar: Author Only Title Only Author and Title

Moseyko, N., and Feldman, L.J. (2001). Expression of pH-sensitive green fluorescent protein in Arabidopsis thaliana. Plant, Cell & Environment 24, 557-563.
Pubmed: Author and Title
Google Scholar: Author Only Title Only Author and Title

Nagai, T., Yamada, S., Tominaga, T., Ichikawa, M., and Miyawaki, A. (2004). Expanded dynamic range of fluorescent indicators for Ca2+ by circularly permuted yellow fluorescent proteins. Proceedings of the National Academy of Sciences of the United States of America 101, 10554-10559.
Pubmed: Author and Title
Google Scholar: Author Only Title Only Author and Title

Okuda, S., Tsutsui, H., Shiina, K., Sprunck, S., Takeuchi, H., Yui, R., Kasahara, R.D., Hamamura, Y., Mizukami, A., Susaki, D., et al. (2009). Defensin-like polypeptide LUREs are pollen tube attractants secreted from synergid cells. Nature 458, 357-361.
Pubmed: Author and Title
Google Scholar: Author Only Title Only Author and Title

Pearce, G., Moura, D.S., Stratmann, J., and Ryan, C.A. (2001). RALF, a 5-kDa ubiquitous polypeptide in plants, arrests root growth and development. Proceedings of the National Academy of Sciences 98, 12843-12847.
Pubmed: Author and Title
Google Scholar: Author Only Title Only Author and Title

Rajasekar, K.V., Ji, S., Coulthard, R.J., Ride, J.P., Reynolds, G.L., Winn, P.J., Wheeler, M.J., Hyde, E.I., and Smith, L.J. (2019). Structure of SPH (self-incompatibility protein homologue) proteins: a widespread family of small, highly stable, secreted proteins. Biochemical Journal 476, 809-826.

Pubmed: Author and Title
Google Scholar: Author Only Title Only Author and Title

Ride, J.P., Davies, E.M., Franklin, F.C.H., and Marshall, D.F. (1999). Analysis of Arabidopsis genome sequence reveals a large new gene family in plants. Plant Molecular Biology 39, 927-932.
Pubmed: Author and Title
Google Scholar: Author Only Title Only Author and Title

Schopfer, C.R., Nasrallah, M.E., and Nasrallah, J.B. (1999). The male determinant of self-incompatibility in Brassica. Science 286, 1697-1700.
Pubmed: Author and Title
Google Scholar: Author Only Title Only Author and Title

Silverstein, K.A.T., Moskal Jr., W.A., Wu, H.C., Underwood, B.A., Graham, M.A., Town, C.D., and VandenBosch, K.A. (2007). Small cysteine-rich peptides resembling antimicrobial peptides have been under-predicted in plants. The Plant Journal 51, 262-280.
Pubmed: Author and Title
Google Scholar: Author Only Title Only Author and Title

Snowman, B.N., Kovar, D.R., Shevchenko, G., Franklin-Tong, V.E., and Staiger, C.J. (2002). Signal-mediated depolymerization of actin in pollen during the self-incompatibility response. The Plant Cell 14, 2613-2626.
Pubmed: Author and Title
Google Scholar: Author Only Title Only Author and Title

Sparks, E., Wachsman, G., and Benfey, P.N. (2013). Spatiotemporal signalling in plant development. Nat Rev Genet 14, 631-644.
Pubmed: Author and Title
Google Scholar: Author Only Title Only Author and Title

Szklarczyk, D., Gable, A.L., Lyon, D., Junge, A., Wyder, S., Huerta-Cepas, J., Simonovic, M., Doncheva, N.T., Morris, J.H., Bork, P., et al. (2019). STRING v11: protein-protein association networks with increased coverage, supporting functional discovery in genome-wide experimental datasets. Nucleic acids research 47, D607-d613.
Pubmed: Author and Title
Google Scholar: Author Only Title Only Author and Title

Takayama, S., and Isogai, A. (2005). Self-incompatibility in plants. Annual Review of Plant Biology 56, 467-489.
Pubmed: Author and Title
Google Scholar: Author Only Title Only Author and Title

Takayama, S., Shiba, H., Iwano, M., Shimosato, H., Che, F.-S., Kai, N., Watanabe, M., Suzuki, G., Hinata, K., and Isogai, A. (2000). The pollen determinant of self-incompatibility in Brassica campetris. Proceedings of the National Academy of Sciences 97, 1920-1925.
Pubmed: Author and Title
Google Scholar: Author Only Title Only Author and Title

Takeuchi, H., and Higashiyama, T. (2016). Tip-localized receptors control pollen tube growth and LURE sensing in Arabidopsis. Nature 531, 245-248.
Pubmed: Author and Title
Google Scholar: Author Only Title Only Author and Title

Thomas, S.G., and Franklin-Tong, V.E. (2004). Self-incompatibility triggers programmed cell death in Papaver pollen. Nature 429, 305-309.
Pubmed: Author and Title
Google Scholar: Author Only Title Only Author and Title

Wang, L., Lin, Z., Trivino, M., Nowack, M.K., Franklin-Tong, V.E., and Bosch, M. (2019). Self-incompatibility in Papaver pollen: programmed cell death in an acidic environment. J Exp Bot 70, 2113-2123.
Pubmed: Author and Title
Google Scholar: Author Only Title Only Author and Title

Wang, L., Triviño, M., Lin, Z., Carli, J., Eaves, D.J., Van Damme, D., Nowack, M.K., Franklin-Tong, V.E., and Bosch, M. (2020). New opportunities and insights into Papaver self-incompatibility by imaging engineered Arabidopsis pollen. Journal of Experimental Botany 71, 2451-2463.
Pubmed: Author and Title
Google Scholar: Author Only Title Only Author and Title

Wheeler, M.J., de Graaf, B.H., Hadjiosif, N., Perry, R.M., Poulter, N.S., Osman, K., Vatovec, S., Harper, A., Franklin, F.C., and Franklin-Tong, V.E. (2009). Identification of the pollen self-incompatibility determinant in Papaver rhoeas. Nature 459, 992-995.
Pubmed: Author and Title
Google Scholar: Author Only Title Only Author and Title

Wheeler, M.J., Vatovec, S., and Franklin-Tong, V.E. (2010). The pollen S-determinant in Papaver: comparisons with known plant receptors and protein ligand partners. Journal of Experimental Botany 61, 2015-2025.
Pubmed: Author and Title
Google Scholar: Author Only Title Only Author and Title

Wilkins, K.A., Bancroft, J., Bosch, M., Ings, J., Smirnoff, N., and Franklin-Tong, V.E. (2011). Reactive Oxygen Species and Nitric Oxide Mediate Actin Reorganization and Programmed Cell Death in the Self-Incompatibility Response of *Papaver*. Plant Physiol 156, 404-416.

Pubmed: Author and Title
Google Scholar: Author Only Title Only Author and Title

Wilkins, K.A., Bosch, M., Haque, T., Teng, N., Poulter, N.S., and Franklin-Tong, V.E. (2015). Self-Incompatibility-Induced Programmed Cell Death in Field Poppy Pollen Involves Dramatic Acidification of the Incompatible Pollen Tube Cytosol. Plant Physiol 167, 766-779.
Pubmed: Author and Title
Google Scholar: Author Only Title Only Author and Title

Wilkins, K.A., Poulter, N.S., and Franklin-Tong, V.E. (2014). Taking one for the team: self-recognition and cell suicide in pollen. Journal of Experimental Botany 65, 1331-1342.
Pubmed: Author and Title
Google Scholar: Author Only Title Only Author and Title

Wu, F.-H., Shen, S.-C., Lee, L.-Y., Lee, S.-H., Chan, M.-T., and Lin, C.-S. (2009). Tape-Arabidopsis Sandwich - a simpler Arabidopsis protoplast isolation method. Plant Methods 5, 16.
Pubmed: Author and Title
Google Scholar: Author Only Title Only Author and Title

Yang, Z. (2008). Cell polarity signaling in Arabidopsis. Annual review of cell and developmental biology 24, 551-575.
Pubmed: Author and Title
Google Scholar: Author Only Title Only Author and Title